Systems/Circuits

Dopamine Release in Nucleus Accumbens Is under Tonic Inhibition by Adenosine A_1 Receptors Regulated by Astrocytic ENT1 and Dysregulated by Ethanol

Bradley M. Roberts,[1,2] Elizabeth Lambert,[1] Jessica A. Livesey,[1] Zhaofa Wu,[3] Yulong Li,[3] and Stephanie J. Cragg[1,2]

[1]Centre for Cellular and Molecular Neurobiology, Department of Physiology, Anatomy and Genetics, University of Oxford, Oxford OX1 3PT, United Kingdom, [2]Oxford Parkinson's Disease Centre, University of Oxford, Oxford OX1 3PT, United Kingdom, and [3]State Key Laboratory of Membrane Biology, School of Life Sciences, Peking University, Beijing 100871, People's Republic of China

Striatal adenosine A_1 receptor (A_1R) activation can inhibit dopamine release. A_1Rs on other striatal neurons are activated by an adenosine tone that is limited by equilibrative nucleoside transporter 1 (ENT1) that is enriched on astrocytes and is ethanol sensitive. We explored whether dopamine release in nucleus accumbens core is under tonic inhibition by A_1Rs, and is regulated by astrocytic ENT1 and ethanol. In *ex vivo* striatal slices from male and female mice, A_1R agonists inhibited dopamine release evoked electrically or optogenetically and detected using fast-scan cyclic voltammetry, most strongly for lower stimulation frequencies and pulse numbers, thereby enhancing the activity-dependent contrast of dopamine release. Conversely, A_1R antagonists reduced activity-dependent contrast but enhanced evoked dopamine release levels, even for single optogenetic pulses indicating an underlying tonic inhibition. The ENT1 inhibitor nitrobenzylthioinosine reduced dopamine release and promoted A_1R-mediated inhibition, and, conversely, virally mediated astrocytic overexpression of ENT1 enhanced dopamine release and relieved A_1R-mediated inhibition. By imaging the genetically encoded fluorescent adenosine sensor [GPCR-activation based (GRAB)-Ado], we identified a striatal extracellular adenosine tone that was elevated by the ENT1 inhibitor and sensitive to gliotoxin fluorocitrate. Finally, we identified that ethanol (50 mM) promoted A_1R-mediated inhibition of dopamine release, through diminishing adenosine uptake via ENT1. Together, these data reveal that dopamine output dynamics are gated by a striatal adenosine tone, limiting amplitude but promoting contrast, regulated by ENT1, and promoted by ethanol. These data add to the diverse mechanisms through which ethanol modulates striatal dopamine, and to emerging datasets supporting astrocytic transporters as important regulators of striatal function.

Key words: adenosine; astrocytes; dopamine; equilibrative nucleoside transporter 1; ethanol; tonic inhibition

Significance Statement

Dopamine axons in the mammalian striatum are emerging as strategic sites where neuromodulators can powerfully influence dopamine output in health and disease. We found that ambient levels of the neuromodulator adenosine tonically inhibit dopamine release in nucleus accumbens core via adenosine A_1 receptors (A_1Rs), to a variable level that promotes the contrast in dopamine signals released by different frequencies of activity. We reveal that the equilibrative nucleoside transporter 1 (ENT1) on astrocytes limits this tonic inhibition, and that ethanol promotes it by diminishing adenosine uptake via ENT1. These findings support the hypotheses that A_1Rs on dopamine axons inhibit dopamine release and, furthermore, that astrocytes perform important roles in setting the level of striatal dopamine output, in health and disease.

Received July 28, 2021; revised Nov. 20, 2021; accepted Nov. 23, 2021.

Author contributions: B.M.R. and S.J.C. designed research; B.M.R., E.L., and J.A.L. performed research; Z.W. and Y.L. contributed unpublished reagents/analytic tools; B.M.R., E.L., and J.A.L. analyzed data; B.M.R. and S.J.C. wrote the paper.

This work was supported by UK Medical Research Council Grant MR/V013599/1 (to S.J.C. and B.M.R.); University of Oxford John Fell Fund Grant 0008310 (to B.M.R.); a Junior Research Fellowship to B.M.R. from St John's College, Oxford University; and a Biotechnology and Biological Sciences Research Council Doctoral Training grant to J.A.L.

The authors declare no competing financial interests.

Correspondence should be addressed to Stephanie J. Cragg at Stephanie.Cragg@dpag.ox.ac.uk or Bradley M. Roberts at Bradley.Roberts@dpag.ox.ac.uk.

https://doi.org/10.1523/JNEUROSCI.1548-21.2021

Introduction

Striatal dopamine (DA) axons are major strategic sites for striatal neuromodulators to influence DA output (Rice et al., 2011; Sulzer et al., 2016; Nolan et al., 2020; Roberts et al., 2021). Adenosine acts at A_1 receptors (A_1Rs) and $A_{2A}Rs$ on diverse neurons in striatum, and exogenous activation of striatal A_1Rs, but not A_2Rs, inhibit evoked DA release (Okada et al., 1996; O'Neill et al., 2007; O'Connor and O'Neill, 2008; Ross and Venton, 2015). Immunocytochemical studies of rat synaptosomes suggest that A_1Rs can be localized directly to striatal DA

Table 1. Comparison of effects of adenosine A_1 receptor agonists and antagonists on evoked mean peak $[DA]_o$ between sexes

Sex	Mean $[DA]_o$ (% predrug)	SEM	*N*	Unpaired *t* test
Figure 1*B*: A_1 agonist (CPA), electrically evoked DA release				
Male	39.6	6.8	3	$t_{(4)} = 0.467$, $p = 0.665$
Female	43.2	3.9	3	
Figure 1*G*: A_1 agonist (CPA), optogenetically evoked DA release				
Male	59.4	2.9	4	$t_{(6)} = 1.141$, $p = 0.297$
Female	53.4	4.4	4	
Figure 3*A*: A_1 antagonist (CPT), electrically evoked DA release				
Male	140.8	7.8	4	$t_{(5)} = 0.181$, $p = 0.864$
Female	142.6	5.4	3	
Figure 3*C*: A_1 antagonist (caffeine), electrically evoked DA release				
Male	117.4	8.0	3	$t_{(4)} = 0.304$, $p = 0.777$
Female	114.9	2.2	3	
Figure 3*E*: A_1 antagonist (CPT), optogenetically evoked DA release				
Male	126.6	16.7	3	$t_{(6)} = 0.258$, $p = 0.805$
Female	130.0	3.8	5	

axons (Borycz et al., 2007), but definitive evidence is lacking and other intermediary inputs to DA axons have not been excluded. In nucleus accumbens core (NAcC), adenosine can provide tonic A_1R-mediated inhibition of glutamatergic and GABAergic transmission (Brundege and Williams, 2002; Adhikary and Birdsong, 2021). DA release in NAcC and caudate–putamen has been suggested to be under tonic A_1R-mediated inhibition, as A_1R antagonists increase extracellular DA levels in rats *in vivo* measured by microdialysis (Okada et al., 1996; Solinas et al., 2002; Quarta et al., 2004a, b; Borycz et al., 2007), but whether these effects were direct and local or involved intact long-loop circuits was not resolved. Furthermore, adenosine acts in a frequency-dependent manner on glutamate and GABA transmission across other nuclei, resulting in a stronger A_1R-dependent inhibition of neurotransmission elicited by low-frequency versus high-frequency electrical stimulations (e.g., neocortex: Yang et al., 2007; Qi et al., 2017; Perrier et al., 2019; hippocampus: Moore et al., 2003; calyx of Held: Wong et al., 2006). It has not yet been established whether striatal A_1Rs simply inhibit DA neurotransmission, or might also promote contrast in DA signals released by different firing rates, and whether in turn this is independent from striatal acetylcholine (ACh) or GABA circuits, which modify DA signal contrast (Rice and Cragg, 2004; Lopes et al., 2019).

Extracellular adenosine concentrations are limited by the activity of nucleoside transporters, most notably the equilibrative nucleoside transporter type 1 (ENT1; Young et al., 2008; Nguyen et al., 2015). ENT1 is expressed in striatum (Anderson et al., 1999; Jennings et al., 2001) and is especially abundant on astrocytes (Peng et al., 2005; Chai et al., 2017). ENT1 on astrocytes can regulate adenosine signaling in striatum and elsewhere (Nagai et al., 2005; Tanaka et al., 2011; Boddum et al., 2016; Cheffer et al., 2018; Hong et al., 2020), and in dorsal striatum, astrocytic ENT1 activity modulates reward-seeking behaviors (Hong et al., 2020; Kang et al., 2020). We recently identified that astrocytes regulate DA release, because of their expression of GABA transporters that regulate tonic GABAergic inhibition (Roberts et al., 2020), but whether ENT1 on astrocytes also modulates DA output by regulating adenosine tone at A_1Rs has not been explored. Additionally, adenosine uptake by ENT1 is impaired by acute ethanol, which augments extracellular adenosine levels (Nagy et al., 1989, 1990; Choi et al., 2004) and contributes to the ataxic and hypnotic effects of ethanol through the activation of striatal A_1Rs (Meng and Dar, 1995; Phan et al., 1997; Dar, 2001). Acute ethanol reduces DA release evoked in NAcC in brain slices (Yorgason et al., 2014, 2015), as does chronic intermittent ethanol exposure in mice (Karkhanis et al., 2015; Rose et al., 2016), raising the question of whether ethanol regulates DA by promoting A_1R-mediated inhibition of DA release.

Here, we assessed A_1R regulation of DA release in NAcC by detecting DA in real time using fast-scan cyclic voltammetry and detecting striatal adenosine using the genetically encoded fluorescent adenosine sensor [GPCR-activation based (GRAB)-Ado; Peng et al., 2020; Wu et al., 2020]. We reveal that A_1Rs can tonically inhibit DA output though an ambient adenosine tone, and that A_1Rs additionally regulate the activity sensitivity of DA release, independently from striatal acetylcholine or GABA inputs. Furthermore, we find that tonic A_1R-mediated inhibition of DA release is regulated by adenosine uptake by ENT1 on astrocytes, and is dysregulated by ethanol.

Materials and Methods

Animals. All procedures were performed in accordance with the Animals in Scientific Procedures Act 1986 (Amended 2012) with ethical approval from the University of Oxford, and under authority of a Project License granted by the UK Home Office. Experiments were conducted using male and female adult (6- to 12-week-old) C57BL/6J mice (Charles River) or heterozygote knock-in mice bearing an internal ribosome entry site (IRES)-linked Cre recombinase gene downstream of the gene *Slc6a3*, which encodes the plasma membrane DA transporter (*Slc6a3*$^{IRES\text{-}Cre}$ mice; *B6.SJL-Slc6a3*$^{tm1.1(cre)Bkmn}$/J, stock #006660, The Jackson Laboratory) maintained on a C57BL/6J background. All mice were group housed and maintained on a 12 h light/dark cycle (light ON from 7:00 A.M. to 7:00 P.M.) with *ad libitum* access to food and water. Data from male and female mice were combined throughout as no differences in the effects of adenosine A_1 receptor agonists or antagonists between sexes were observed (Table 1).

Stereotaxic intracranial injections. Mice were anesthetized with isoflurane and placed in a small animal stereotaxic frame (David Kopf Instruments). After exposing the skull under aseptic techniques, a small burr hole was drilled and adeno-associated viral solutions were injected at an infusion rate of 100 nl/min with a 32 gauge syringe (Hamilton) using a microsyringe pump (World Precision Instruments) and were withdrawn 5 min after the end of injection. To virally express channelrhodopsin-2 (ChR2) selectively in DA neurons, 600 nl/hemisphere AAV5-EF1α-DIO-hChR2(H134R)-eYFP (8×10^{12} genome copies/ml; UNC Vector Core Facility) encoding Cre-dependent ChR2 was injected bilaterally into the midbrain [anteroposterior (AP), −3.1 mm; mediolateral (ML), ±1.2 mm from bregma; dorsoventral (DV), −4.25 mm from exposed dura mater] of 6-week-old *Slc6a3*$^{IRES\text{-}Cre}$ mice, following previously described methods (Roberts et al., 2020). To overexpress ENT1 in striatal astrocytes, 600 nl/hemisphere AAV5-GfaABC$_1$D-mENT1/mCherry-WPRE (1.6×10^{13} genome copies/ml; VECTOR BIOLABS)

encoding a fluorescence protein-fused and functional ENT1 under the astrocyte-specific abbreviated glial fibrillary acidic protein promoter (*GfaABC$_1$D*; Hong et al., 2020; Jia et al., 2020) or AAV5-GfaABC$_1$D-mCherry-WPRE (6.1×10^{12} genome copies/ml; ETH Zurich Viral Vector Facility) for control fluorophore expression, was injected bilaterally into nucleus accumbens (AP, +1.3 mm; ML, ±1.2 mm from bregma; DV, −3.75 mm from exposed dura mater) of 6-week-old C57BL/6J wild-type mice. To virally express the fluorescent adenosine reporter GRAB-Ado (Peng et al., 2020; Wu et al., 2020), 800 nl/hemisphere AAV9-hSyn-GRAB-Ado1.0m (0.5×10^{13} genome copies/ml; WZ Biosciences) was injected bilaterally into nucleus accumbens or dorsal striatum (AP, +0.8 mm; ML, ±1.75 mm from bregma; DV, −2.40 mm from exposed dura mater) of 6-week-old C57BL/6J wild-type mice. Mice were used for experiments 2−4 weeks post-intracranial injection.

Brain slice preparation. Acute brain slices were obtained from 8- to 12-week-old mice using standard techniques. Mice were culled by cervical dislocation within 1−2 h after the start of the light-ON period of the light cycle, and brains were dissected out and submerged in ice-cold cutting solution containing the following (in mM): 194 sucrose, 30 NaCl, 4.5 KCl, 1 $MgCl_2$, 26 $NaHCO_3$, 1.2 NaH_2PO_4, and 10 D-glucose. Coronal slices 300 μm thick containing striatum were prepared from dissected brain tissue using a vibratome (model VT1200S, Leica Microsystems) and transferred to a holding chamber containing artificial CSF (aCSF) containing the following (in mM): 130 NaCl, 2.5 KCl, 26 $NaHCO_3$, 2.5 $CaCl_2$, 2 $MgCl_2$, 1.25 NaH_2PO_4, and 10 glucose. Sections were incubated at 34°C for 15 min before they were stored at room temperature (20–22° C) until recordings were performed. All recordings were obtained within 8 h of slicing. All solutions were saturated with 95% O_2/5% CO_2. Before recording, individual slices were hemisected, transferred to a recording chamber, and superfused at ~2.5–3.0 ml/min with aCSF at 31–33°C.

Fast-scan cyclic voltammetry. Evoked extracellular DA concentration ($[DA]_o$) was measured in acute coronal brain slices using fast-scan cyclic voltammetry (FSCV) at carbon fiber microelectrodes (diameter, 7–10 μm) fabricated in-house (tip length, 70–120 μm) as used previously (Roberts et al., 2020). In brief, a triangular voltage waveform was scanned across the microelectrode (−700 to +1300 mV vs Ag/AgCl reference) at 800 V/s and at a scan frequency of 8 Hz using a Millar Voltammeter (Julian Millar, Barts and the London School of Medicine and Dentistry, London, UK). Microelectrodes were calibrated *post hoc* in 2 μM DA in each experimental solution. Microelectrode sensitivity to DA was between 10 and 40 nA/μM. Signals were attributed to DA because of the potentials of their characteristic oxidation (500–600 mV) and reduction (−200 mV) peaks. Currents at the oxidation peak potential were measured from the baseline of each voltammogram and plotted against time to provide profiles of $[DA]_o$ versus time. Recordings were conducted in the NAcC, within ~100 μm of the anterior commissure, one site per slice. Electrical or light stimuli were delivered at 2.5 min intervals, which allow stable DA release to be sustained at ~90–95% of original levels over the typical time course of experiments, in control conditions (Roberts et al., 2020). In experiments where $[DA]_o$ was evoked by electrical stimulation, a local bipolar concentric Pt/Ir electrode (inner diameter, 25 μm; outer diameter, 125 μm; FHC) was placed ~100 μm from the recording microelectrode and stimulus pulses (duration, 200 μs) were given at 0.6 mA. We applied either a single pulse (1p) or trains of 2–20 pulses at 10–100 Hz. In experiments where $[DA]_o$ was evoked by light stimulation in slices prepared from *Slc6a3$^{IRES\text{-}Cre}$* mice expressing ChR2, DA axons in NAcC were activated by TTL (transistor–transistor logic)-driven (Multi Channel Stimulus II, Multi Channel Systems) brief pulses (2 ms) of blue light (470 nm; 5 mW/mm^2; OptoLED, Cairn Research), which illuminated the field of view (diameter, 2.2 mm; 10× water-immersion objective). Data were digitized at 50 kHz using a Digidata 1550A digitizer (Molecular Devices). Data were acquired and analyzed using Axoscope 11.0 (Molecular Devices) and locally written VBA scripts in Microsoft Excel (2013).

GRAB-Ado imaging. An Olympus BX51WI microscope equipped with a 470 nm OptoLED light system (Cairn Research), Iris 9 Scientific CMOS camera (Teledyne Photometrics), 525/50 nm emission filter (Cairn Research), and 10×/0.3 numerical aperture water-immersion objective (Olympus) was used for wide-field fluorescence imaging of GRAB-Ado in striatal slices. Image acquisition was controlled using Micro-Manager 1.4. Electrical stimulation, LED light, and image acquisition were synchronized using TTL-driven stimuli via Multi Channel Stimulus II (Multi Channel Systems). Image files were analyzed with MATLAB R2017b and Fiji 1.5. For experiments measuring changes to basal, nonstimulated extracellular adenosine levels, images (exposure duration, 100 ms) were acquired every 30 s during brief exposure (1 s) to blue light (470 nm; 1 mW/mm^2; OptoLED, Cairn Research) for a 40 min window. We extracted fluorescence intensity from the region of interest (ROI; 150 × 150 μm) and derived a background-subtracted fluorescence intensity (F_t) by subtracting background fluorescence intensity from an equal-sized ROI where there was no GRAB-Ado expression (i.e., cortex). Data are expressed as a change in fluorescence ($\Delta F/F_0$) and were derived by calculating $[(F_t - F_0)/F_0]$, where F_0 is the average F_t of the first 20 acquired images (initial 10 min). For experiments measuring extracellular adenosine levels in response to trains of electrical stimulation or experiments calibrating GRAB-Ado signals to applications of known concentrations of exogenous adenosine, images were acquired at 10 Hz (exposure duration, 100 ms) during continuous blue light (470 nm; 1 mW/mm^2; OptoLED, Cairn Research) for a 4 min recording window. For evoked adenosine release, electrical stimulus pulses (100 pulses at 50 Hz; pulse duration, 200 μs; 0.6 mA) were given by a local bipolar concentric Pt/Ir electrode (inner diameter, 25 μm; outer diameter, 125 μm; FHC) at the 30 s time point. Bath applications of exogenous adenosine were also applied at the 30 s time point. F_t was extracted from an ROI (150 × 150 μm) ~50 μm from the stimulating electrode, and $\Delta F/F_0$ was derived by calculating $[(F_t - F_0)/F_0]$, where F_0 is the average fluorescence intensity over the 10 s window (100 images) before onset of electrical stimulation or bath application of exogenous adenosine.

Drugs. Adenosine (25–100 μM), (+)-bicuculline (10 μM), dihydro-β-erythroidine hydrobromide (DHβE; 1 μM), nitrobenzylthioinosine (NBTI; 10 μM), and tetrodotoxin (TTX; 1 μM) were obtained from Tocris Bioscience. CGP 55845 hydrochloride (CGP; 4 μM), 8-cyclopentyl-1,3-dimethylxanthine (CPT; 10 μM), and dipropylcyclopentylxanthine (DPCPX; 2 μM) were obtained from Abcam. Ethanol (EtOH; 50 mM), and N^6-cyclopentyladenosine (CPA; 15 μM) were obtained from Sigma-Aldrich. Fluorocitrate (FC) was prepared as previously described (Paulsen et al., 1987; Roberts et al., 2020). In brief, D,L-fluorocitric acid Ba_3 salt (Sigma-Aldrich) was dissolved in 0.1 M HCl, and the Ba^{2+} was precipitated with 0.1 M Na_2S0_4 and then centrifuged at 1000 × g for 5 min. Supernatant containing fluorocitrate was used at a final concentration of 100 μM for experimentation.

Immunocytochemistry. To confirm viral ENT1-mCherry expression in non-neuronal cells, direct mCherry fluorophore expression was compared with indirect immunofluorescence for neuronal marker NeuN. ENT1-mCherry-expressing mice were anesthetized with an overdose of pentobarbital and was transcardially perfused with PBS, followed by 4% paraformaldehyde (PFA) in 0.1 M phosphate buffer, pH 7.4. Brains were removed and postfixed overnight in 4% PFA. Coronal sections were cut using a vibrating microtome (model VT1000S, Leica) at a thickness of 50 µm and collected in a 1 in 4 series. Sections were stored in PBS with 0.05% sodium azide until processing. Upon processing, sections were washed in PBS and then blocked for 1 h in a solution of PBS Triton X-100 (0.3%; PBS-Tx) containing 10% normal donkey serum (NDS). Sections were then incubated in primary antibodies overnight in PBS-Tx with 2% NDS at 4°C. The primary antibody used was rabbit anti-NeuN (1:500; catalog #R-3770–100, BIOSENSIS). Sections were then incubated in species-appropriate fluorescent secondary antibodies with minimal cross-reactivity for 2 h in PBS-Tx with 2% NDS at room temperature. The secondary antibody used was donkey anti-rabbit Alexa Fluor 405 (1:500; catalog #ab175651, Abcam). Sections were washed in PBS and then mounted on glass slides and coverslipped using Vectashield (Vector Laboratories). Coverslips were sealed using nail varnish and stored at 4°C. Confocal images were acquired with a confocal laser-scanning microscope (model FV3000, Olympus) using a 20× and 40× objective and filters for appropriate excitation and emission wave lengths (Olympus Medical).

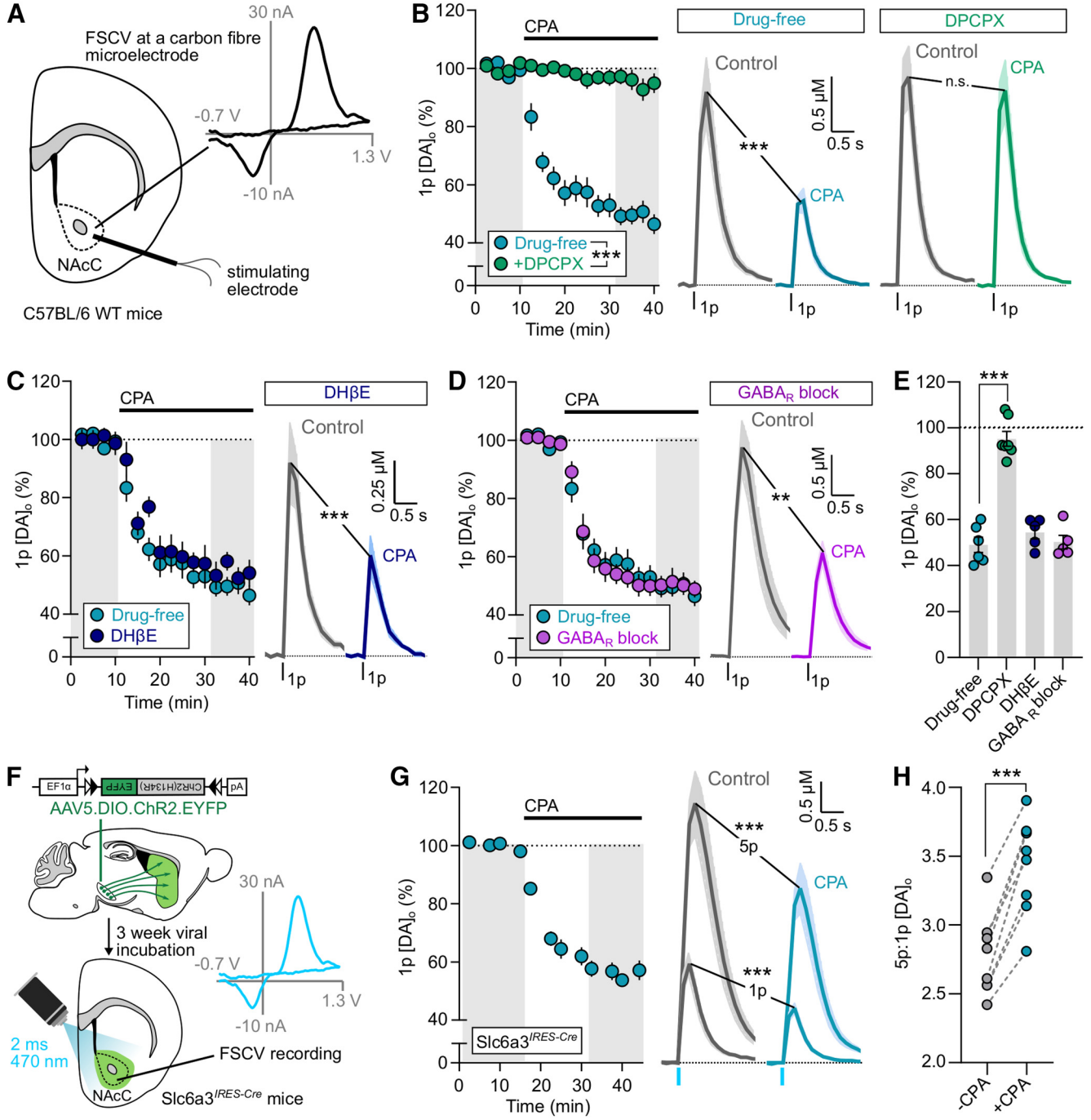

Figure 1. Adenosine A_1R agonists inhibit DA release in NAcC. ***A***, Experimental setup for FSCV for DA detection in wild-type mouse NAcC in acute slices. Inset, Typical evoked DA voltammogram. ***B–D***, Left, Summary of mean peak $[DA]_o$ evoked by a 1p before and after application of A_1R agonist CPA (15 μM) normalized to predrug baseline level (dotted line). Shaded areas represent time points used to obtain data on right, mean $[DA]_o$ transients in either drug-free ACSF (blue $n = 6$ experiments/4 mice), or in the presence of A_1R antagonist DPCPX (2 μM; green, $n = 8$ experiments/5 mice; ***B***) or nAChR antagonist DHβE (1 μM; dark blue, $n = 5$ experiments/4 mice; ***C***), or $GABA_A$ and $GABA_B$ antagonists (+)-bicuculline (10 μM) and CGP 55 845 (4 μM; purple, $n = 5$ experiments/4 mice; ***D***). Control data in ***C*** and ***D*** are from ***B***. ***E***, Mean peak $[DA]_o$ following application of CPA (15 μM; as a percentage of predrug baseline, data are summarized from ***B–D***). ***F***, Viral injection into midbrain of Slc6a3$^{IRES\text{-}Cre}$ mice for the expression of ChR2-eYFP in DA axons for optogenetic-evoked DA release. ***G***, As in ***B*** but $[DA]_o$ evoked optogenetically by 1p or 5p of light at 25 Hz ($n = 8$ experiments/5 mice). ***H***, Ratio of peak $[DA]_o$ evoked by 5p:1p ratio at 25 Hz before (gray) and after (blue) application of CPA (15 μM). ***$p < 0.001$, paired *t* tests (***B–D***, ***G***, ***H***), unpaired *t* tests (***E***), and two-way repeated-measures ANOVA (***B–D***). Error bars indicate SEM.

Results

Adenosine A_1Rs inhibit striatal DA release

Previous studies have shown that agonists for striatal A_1Rs inhibit DA release evoked by discrete electrical stimulations in dorsal and ventral striatum (O'Neill et al., 2007; O'Connor and O'Neill, 2008; Ross and Venton, 2015). We first corroborated these observations in NAcC for DA release evoked by single stimulus pulses and detected using FSCV in *ex vivo* coronal slices (Fig. 1*A*). Bath application of A_1R agonist CPA (15 μM) reduced evoked $[DA]_o$ by ~50% (Fig. 1*B*; $t_{(5)} = 15.2$, $p < 0.0001$, paired *t* test). This effect of CPA was prevented by prior application of A_1R antagonist DPCPX [2 μM; Fig. 1*B*; $F_{(1,11)} = 88.6$, $p < 0.0001$, two-way repeated-measures (RM) ANOVA for the effect of CPA in

the absence vs presence of DPCPX; Fig. 1*E*; $t_{(11)} = 9.99$, $p < 0.0001$, unpaired *t* test], confirming an action via A_1Rs.

Striatal cholinergic interneurons (ChIs) have A_1Rs (Alexander and Reddington, 1989; Ferré et al., 1996; Preston et al., 2000; Song et al., 2000) through which A_1R agonists can hyperpolarize ChIs and inhibit ACh release (Richardson and Brown, 1987; Brown et al., 1990; Preston et al., 2000). Because ChIs operate strong control over DA release via nAChRs (Jones et al., 2001; Rice and Cragg, 2004; Zhang and Sulzer, 2004) and can mediate the effects of other striatal neuromodulators on DA (Britt and McGehee, 2008; Hartung et al., 2011; Stouffer et al., 2015; Kosillo et al., 2016; Lemos et al., 2019), they might indirectly mediate the control of DA by A_1Rs. We explored whether A_1Rs can modulate striatal DA release in the absence of these potential actions on ChIs and nAChRs. We used nAChR antagonist DHβE (1 μM) to inhibit nAChRs, as described previously (Rice and Cragg, 2004; Threlfell et al., 2012), after which subsequent application of CPA nonetheless reduced $[DA]_o$ evoked by single stimulus pulses by ~50% (Fig. 1*C*; $t_{(4)} = 15.9$, $p < 0.0001$, paired *t* test), an effect not different from that seen in the absence of DHβE (Fig. 1*C*; $F_{(1,9)} = 1.22$, $p = 0.29$, two-way RM ANOVA: main effect of drug; Fig. 1*E*; $t_{(9)} = 1.21$, $p = 0.259$, unpaired *t* test), indicating that A_1Rs can suppress DA release independently from any indirect effects via ChI inputs to nAChRs.

DA release throughout striatum is also under tonic inhibition by GABA through action at $GABA_A$ and $GABA_B$ receptors (Lopes et al., 2019; Roberts et al., 2020), and we tested whether A_1Rs require this GABA input to inhibit DA release. However, in the presence of $GABA_A$ and $GABA_B$ receptor antagonists, bicuculline (10 μM) and CGP 55845 (5 μM), respectively, the A_1R agonist CPA (15 μM) significantly reduced $[DA]_o$ evoked in NAcC by single electrical pulses by ~40% (Fig. 1*D*; $t_{(4)} = 6.10$, $p = 0.0036$, paired *t* test), an effect that was not significantly different from that seen in the absence of GABA receptor antagonists (Fig. 1*D*; $F_{(1,9)} = 0.019$, $p = 0.892$, two-way RM ANOVA: main effect of drug; Fig. 1*E*; $t_{(9)} = 0.259$, $p = 0.802$, unpaired *t* test), indicating that A_1 receptor agonists can inhibit DA release independently from indirect effects acting via striatal GABA modulation of DA.

To further test whether the inhibition of DA release by A_1Rs requires the coactivation of other striatal neuron types or inputs, we tested whether A_1Rs modulate DA release evoked optogenetically by targeted light activation of DA axons. Optogenetic activation of DA axons minimizes the activation of other striatal neurons that occurs with nonselective electrical stimulation; optogenetically evoked DA release is independent of at least nAChR input (Threlfell et al., 2012; Melchior et al., 2015). We expressed ChR2-enhanced yellow fluorescent protein (eYFP) in DA neurons and axons in $Slc6a3^{IRES\text{-}Cre}$ mice using an established viral approach (Fig. 1*F*), as we previously described (Roberts et al., 2020). CPA suppressed $[DA]_o$ evoked in NAcC by single brief (2 ms) blue light pulses (Fig. 1*G*; $t_{(7)} = 16.2$, $p < 0.0001$, paired *t* test), indicating that A_1Rs can inhibit DA release independently from not just ChI input to nAChRs, but also without requiring the coincident activation of inputs from other neuron types, suggesting that A_1R inhibition of DA release could be via direct action on DA axons, although actions via an unidentified tonically active input that is not GABA are possible.

Striatal A_1Rs enhance the frequency and activity sensitivity of DA release

Previous studies exploring whether striatal A_1Rs regulate DA release have predominantly focused on the effects on release evoked by single, discrete stimuli, and impact on release by the full range of physiologically relevant frequencies has not been explored. Adenosine acts in a frequency-dependent manner on glutamate and GABA transmission in other brain nuclei, resulting in a stronger A_1R-dependent inhibition of neurotransmission elicited by low-frequency versus high-frequency electrical stimulations, and therefore operating like a high-pass input filter on neurotransmitter release (e.g., neocortex: Yang et al., 2007; Qi et al., 2017; Perrier et al., 2019; hippocampus: Moore et al., 2003; calyx of Held: Wong et al., 2006). Other inputs and mechanisms that inhibit DA release by single stimuli can also promote the frequency dependence of DA release, for instance GABA (Lopes et al., 2019; Roberts et al., 2020), consistent with a reduction in the initial release probability and a consequent relief of some short-term depression (Condon et al., 2019). Using optogenetic activation, we observed a sizeable enhancement in the 5p:1p ratio (for 25 Hz) of light-evoked $[DA]_o$ in the NAcC following application of CPA (Fig. 1*H*; $t_{(7)} = 10.4$, $p < 0.0001$, paired *t* test), suggesting that striatal A_1Rs might promote the sensitivity of DA release to firing rate.

We used electrical stimulation to investigate the effects of A_1R activation on DA release across a full range of physiological DA neuron firing frequencies (1, 10, 50, and 100 Hz), with varying pulse numbers (5, 10, 15, and 20 p). These experiments were conducted in the presence of nAChR antagonist DHβE (1 μM) to eliminate the effects of ChIs at nAChRs, which profoundly restrict the apparent frequency and activity sensitivity of evoked DA release (Rice and Cragg, 2004; Zhang and Sulzer, 2004). A_1R activation by CPA (15 μM) inhibited DA release inversely and significantly with stimulation frequency (Fig. 2*A*,*B*; $F_{(3,18)} = 53.9$, $p < 0.0001$, one-way RM ANOVA), such that CPA significantly increased the frequency dependence of evoked DA release (Fig. 2*C*; $F_{(1,7)} = 38.2$, $p = 0.0005$, two-way RM ANOVA: main effect of drug; $F_{(3,21)} = 23.0$, $p < 0.0001$, frequency × drug interaction). In addition, A_1R activation by CPA inhibited DA release in a manner that varied inversely with the number of pulses in a train (50 Hz; Fig. 2*D*,*E*; $F_{(6,24)} = 31.1$, $p < 0.0001$, one-way RM ANOVA), which significantly increased the pulse-dependence of evoked DA release (Fig. 2*F*; $F_{(1,7)} = 46.7$, $p = 0.0002$, two-way RM ANOVA: main effect of drug; $F_{(4,28)} = 28.2$, $p < 0.0001$, pulse number × drug interaction). Therefore, striatal A_1Rs do not simply inhibit DA release, but have a dynamic outcome depending on activity, that promotes the contrast in DA signals released by different activity.

Adenosine operates a tonic inhibition on DA release

We next addressed whether A_1Rs provide an endogenous inhibition of DA release levels and support the contrast in DA signals released by different activity. Previous *in vivo* microdialysis studies indicate that endogenous adenosine might even exert a tonic A_1R-mediated inhibition of DA release, as systemic dosing or intrastriatal infusions of A_1R antagonists (as well as competitive A_1 and A_{2A} receptor antagonist caffeine; Solinas et al., 2002; Quarta et al., 2004a) increase extracellular striatal DA levels (Okada et al., 1996; Quarta et al., 2004b; Borycz et al., 2007). These effects might involve indirect actions via long loop circuits that are intact *in vivo* that could modulate DA neuron firing in midbrain. We tested therefore whether endogenous inhibition of DA release by A_1Rs could be localized to the NAcC and whether it occurs without coactivation of other neurons, indicative of an tonic inhibition of DA release, by exploring the effects of A_1R antagonists on DA release in NAcC evoked either electrically or optogenetically in coronal striatal slices.

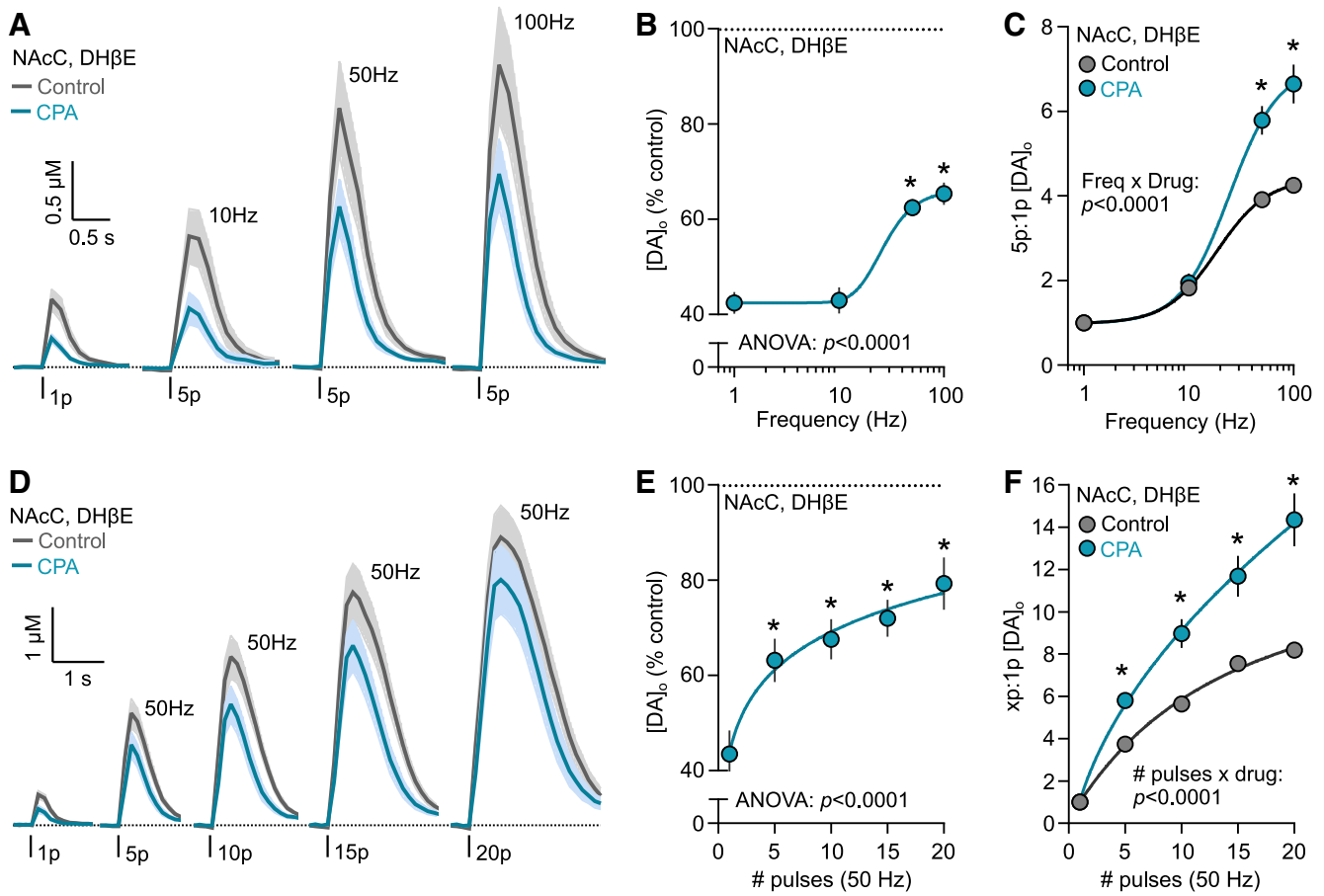

Figure 2. Adenosine A_1R agonists modify the frequency and activity sensitivity of DA release in NAcC. ***A***, Mean $[DA]_o$ transients evoked by one or five electrical pulses in control conditions (gray) or in A_1R agonist CPA (15 μM; blue) in NAcC ($n = 7$ experiments/5 mice). ***B***, Mean peak $[DA]_o$ from ***A*** normalized to control conditions versus stimulation frequency. ***C***, Mean peak $[DA]_o$ from ***A*** normalized to 1p in each condition versus stimulation frequency. ***D***, Mean $[DA]_o$ transient evoked by 1–20 pulses (50 Hz) of electrical trains in control conditions (gray) or in A_1R agonist CPA (15 μM; blue) in NAcC ($n = 7$ experiments/5 mice). ***E***, Mean peak $[DA]_o$ from ***D*** normalized to control conditions versus pulse number. ***F***, Mean peak $[DA]_o$ from ***D*** normalized to 1p in each condition versus number of pulses. *$p < 0.001$, one-way repeated-measures ANOVA with Sidak's multiple comparisons to 1p (***B***, ***E***), two-way repeated-measures ANOVA with Sidak's multiple comparisons (***C***, ***F***). Sigmoidal nonlinear curve fits. Error bars indicate SEM of DHβE (1 μM) present throughout.

Application of the A_1R antagonist CPT (10 μM) significantly enhanced $[DA]_o$ evoked by single or five pulses (50 Hz) of electrical stimulation by ~30–40% (Fig. 3*A*; 1p: $t_{(6)} = 5.10$, $p = 0.0022$; 5p: $t_{(6)} = 5.13$, $p = 0.0022$; paired t tests) and in turn, decreased the ratio of $[DA]_o$ evoked by the 5p:1p ratio (Fig. 3*B*; $t_{(6)} = 3.72$, $p = 0.0099$, paired t test), indicative of an underlying regulation of DA release by endogenous adenosine. Caffeine (20 μM) also significantly enhanced $[DA]_o$ evoked by single or five pulses (50 Hz) of electrical stimulation by ~20–10% (Fig. 3*C*; 1p: $t_{(5)} = 3.69$, $p = 0.014$; 5p: $t_{(5)} = 3.49$, $p = 0.018$; paired t tests) and decreased the ratio of $[DA]_o$ evoked by the 5p:1p ratio (Fig. 3*D*; $t_{(5)} = 3.59$, $p = 0.016$, paired t test). We then investigated whether A_1R-mediated inhibition of DA release by endogenous adenosine might arise through an ambient adenosine tone, by exploring whether A_1R antagonist CPT could promote DA release when evoked using optogenetic stimulation to activate DA axons selectively without coactivation of other striatal cell types that might provide a source of endogenous adenosine. CPT significantly enhanced $[DA]_o$ evoked by single and five pulses (25 Hz) of light in $Slc6a3^{IRES\text{-}Cre}$ ChR2-expressing mice by ~20–30% (Fig. 3*E*; 1p: $t_{(7)} = 5.58$, $p = 0.0008$; 5p: $t_{(7)} = 5.51$, $p = 0.0009$; paired t tests) and decreased the ratio of $[DA]_o$ evoked by the 5p:1p ratio (25 Hz; Fig. 3*F*; $t_{(7)} = 13.50$, $p < 0.0001$, paired t test). These data therefore suggest that striatal DA release is under tonic inhibition by an ambient adenosine tone at A_1Rs, which promotes contrast in DA signals released by different activity.

ENT1 on astrocytes is a regulator of tonic A_1R-mediated inhibition of DA release

We next tested the hypothesis that striatal ENT1 and, by association, astrocytes, by governing ambient adenosine levels (Nagai et al., 2005; Young et al., 2008; Tanaka et al., 2011; Nguyen et al., 2015; Cheffer et al., 2018; Hong et al., 2020), might determine the level of tonic A_1R-mediated inhibition of evoked DA release in NAcC. We first inhibited ENT1 activity by pretreatment of slices with the selective ENT1 inhibitor NBTI (10 μM, for 45–60 min), which has previously been shown to increase adenosine levels in striatum (Pajski and Venton, 2010). ENT1 inhibition itself attenuated $[DA]_o$ evoked by single and five pulses (50 Hz) of electrical stimulation (Fig. 4*A*; 1p: $t_{(12)} = 4.38$, $p = 0.0009$; 5p: $t_{(12)} = 3.02$, $p = 0.0107$; unpaired t tests). Furthermore, after pretreatment with NBTI, the A_1R antagonist CPT (10 μM) enhanced $[DA]_o$ evoked by single electrical pulses to a significantly greater degree than in control slices (Fig. 4*B*; $F_{(1,12)} = 27.17$, $p = 0.0002$, two-way RM ANOVA: main effect of drug). CPT decreased the ratio of $[DA]_o$ evoked by 5p:1p ratio (50 Hz) in both conditions (Fig. 4*C*; $F_{(1,12)} = 35.48$, $p < 0.0001$, two-way RM ANOVA: main effect of drug), but there was a significant statistical interaction

between NBTI and CPT (Fig. 4C; $F_{(1,12)}$ = 9.48, p = 0.0096, two-way RM ANOVA: NBTI × CPT interaction) borne out by a greater decrease in this ratio in slices pretreated with NBTI compared with control slices (Fig. 4D; $t_{(12)}$ = 3.08, p = 0.0096, unpaired t test). These data suggest that ENT1 regulates, and in particular limits, how A_1 receptors tonically inhibit DA release and support its associated activity sensitivity.

We then tested conversely whether an upregulation of ENT1 specifically on astrocytes could diminish the level of endogenous A_1R-mediated inhibition of DA release. We targeted fluorescence-tagged ENT1 to astrocytes in the NAcC (Fig. 4E,F) using a viral approach already validated for striatal astrocytes (Hong et al., 2020; Jia et al., 2020). Astrocyte-targeted ENT1 overexpression (ENT1-OX) increased $[DA]_o$ evoked by single and five pulses (50 Hz) of electrical stimulation compared with targeted mCherry controls (Fig. 4G; 1p: $t_{(15)}$ = 3.29, p = 0.0049; 5p: $t_{(15)}$ = 3.49, p = 0.0033; unpaired t tests). Furthermore, with ENT1-OX, the A_1R antagonist CPT (10 μM) enhanced $[DA]_o$ evoked by single electrical pulses to a significantly lesser degree than in mCherry controls (Fig. 4H; $F_{(1,15)}$ = 20.12, p = 0.0004, two-way RM ANOVA: main effect of drug). CPT decreased the ratio of $[DA]_o$ evoked by 5p:1p (50 Hz) in ENT1-OX and mCherry controls (Fig. 4I; $F_{(1,15)}$ = 46.28, p < 0.0001, two-way RM ANOVA: main effect of drug), but there was a significant statistical interaction between ENT1-OX and CPT (Fig. 4I; $F_{(1,15)}$ = 9.54, p = 0.0075, two-way RM ANOVA: ENT1-OX × CPT interaction), which was borne out by a smaller decrease in this ratio following CPT application in ENT1-OX than in controls (Fig. 4J; $t_{(15)}$ = 3.09, p = 0.0075, unpaired t test). Together, these data suggest that ENT1 on astrocytes in particular can support adenosine uptake and set the level of inhibition and regulation of activity dependence of DA release by ambient adenosine acting at A_1Rs.

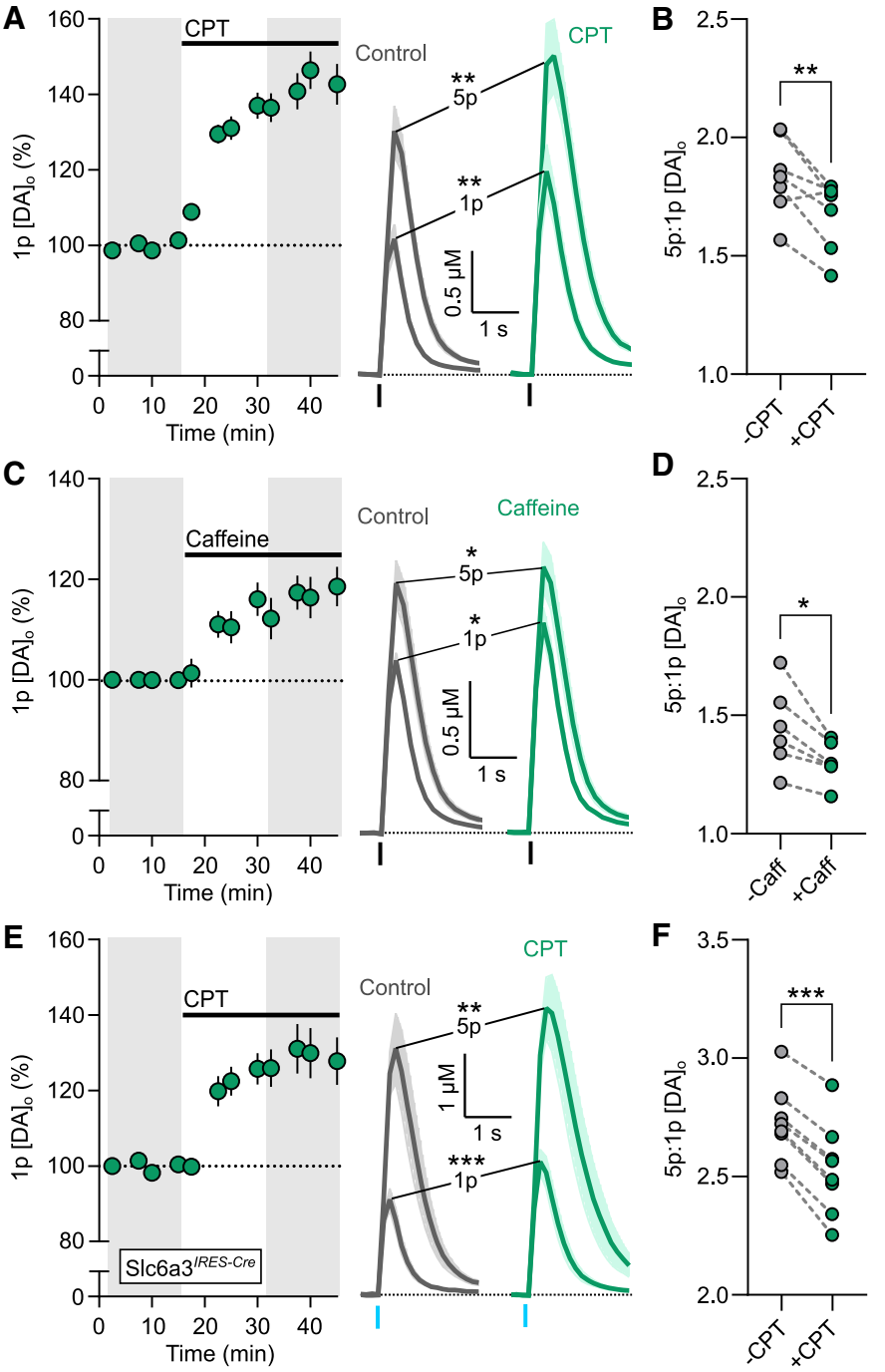

Figure 3. Adenosine A_1R antagonists enhance DA release and correspondingly reduce the activity sensitivity of DA release in NAcC. ***A***, Left, Summary of mean peak $[DA]_o$ before (gray) and after the application of A_1R antagonist CPT (10 μM; green) normalized to predrug baseline (dotted line) and right, corresponding mean $[DA]_o$ transients evoked by 1p and 5p at 50 Hz in NAcC (n = 7 experiments/4 mice). Shaded areas are used to obtain illustrated transients of $[DA]_o$ and for statistical comparisons. ***B***, Ratio of peak $[DA]_o$ evoked by 5p:1p ratio at 50 Hz before (gray) and after (blue) application of CPT (10 μM). Data summarized from ***A***. ***C***, ***D***, As in ***A*** and ***B***, but before (gray) and after (green) application caffeine (20 μM; n = 6 experiments/4 mice). ***E***, ***F***, As in ***A*** and ***B***, but $[DA]_o$ evoked optogenetically by 1p or 5p of light at 25 Hz in $Slc6a3^{IRES\text{-}Cre}$ mice (n = 8 experiments/5 mice). *p < 0.05, **p < 0.01, ***p < 0.001, paired t tests. Error bars indicate SEM.

To resolve directly whether ENT1, and astrocytes, govern striatal adenosine levels, we detected adenosine levels by imaging the recently developed GRAB-Ado sensor (Peng et al., 2020; Wu et al., 2020), a virally expressed genetic reporter, injected into striatum (Fig. 5A). We confirmed that striatal GRAB-Ado sensor fluorescence responded to adenosine concentrations in a concentration-dependent manner on application of exogenous adenosine to slices (Fig. 5B; $F_{(3,35)}$ = 28.73, p < 0.0001, one-way ANOVA), and with a large range of dF/F. To assess the impact of ENT1 on ambient adenosine tone in NAcC, we imaged GRAB-Ado fluorescence before and after ENT1 inhibition, in the absence of any stimulation. Bath application of ENT1 inhibitor NBTI (10 μM) increased fluorescence compared with vehicle controls (Fig. 5C; $F_{(1,18)}$ = 57.8, p < 0.0001, two-way RM ANOVA: main effect of NBTI), indicating that ENT1 limits extracellular adenosine levels. To test whether ENT1 on astrocytes

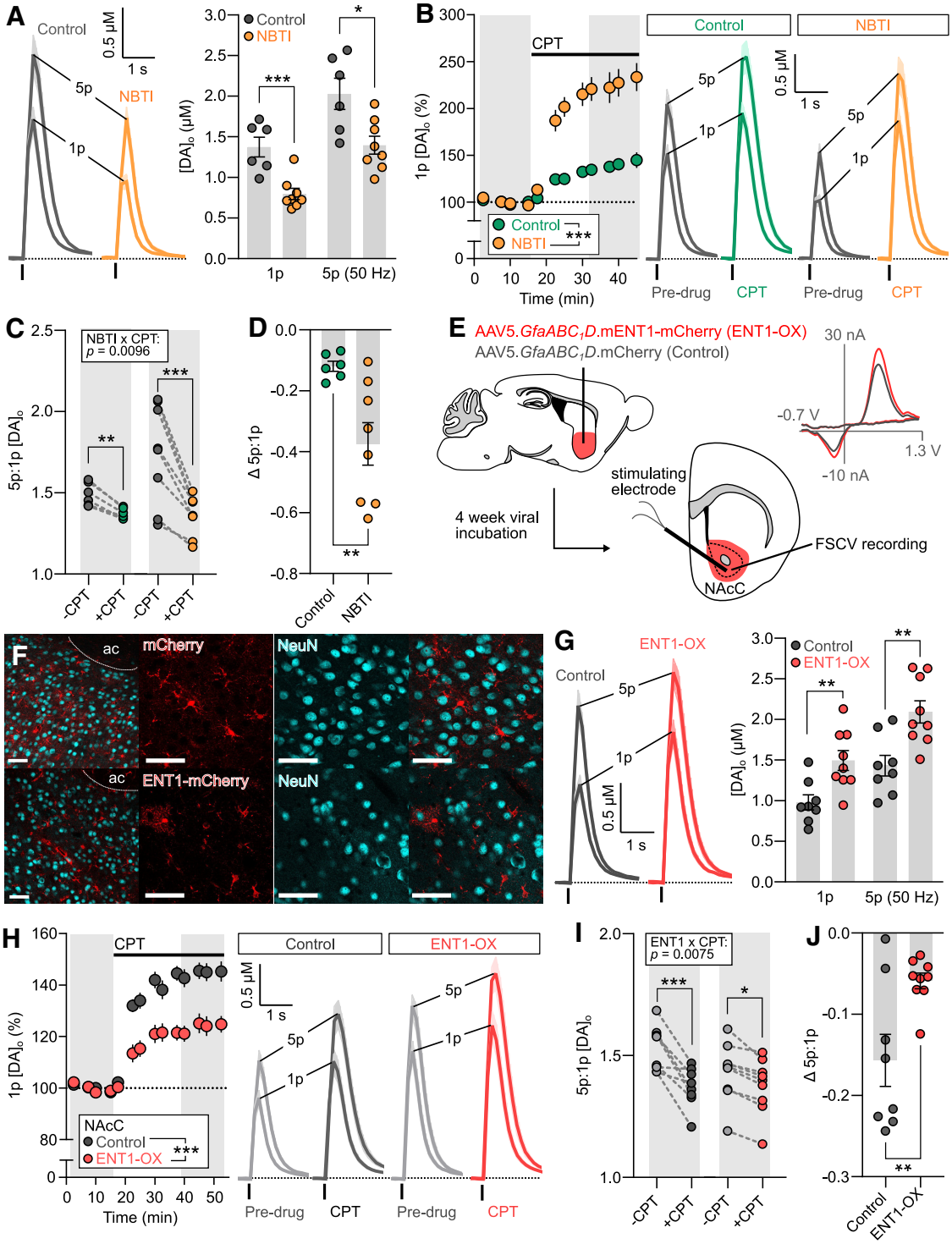

Figure 4. Adenosine uptake by ENT1 on striatal astrocytes regulates tonic A_1R-mediated inhibition of DA release. ***A***, Mean $[DA]_o$ transients (left) and corresponding mean peak $[DA]_o$ (right) evoked by a 1p or 5p at 50 Hz in NAcC in the absence (gray; $n = 6$ experiments/5 mice) or the presence of ENT1 inhibitor NBTI (10 μM; orange; $n = 8$ experiments/5 mice). ***B***, Summary of mean peak $[DA]_o$ before (gray) and after application of A_1R antagonist CPT (10 μM) normalized to predrug baseline level (dotted line; left) and right, corresponding mean $[DA]_o$ transients evoked by 1p and 5p at 50 Hz in NAcC in the absence (green; $n = 6$ experiments/5 mice) or the presence of ENT1 inhibitor NBTI (10 μM; orange; $n = 8$ experiments/5 mice). ***C***, ***D***, Ratio of peak $[DA]_o$ evoked by 5p:1p ratio at 50 Hz (***C***) and Δ5p:1p ratio (***D***) before (gray) and after application of CPT (10 μM) in the absence (left, green) or presence of ENT1 inhibitor NBTI (10 μM; right, orange). Data are summarized from ***B***. ***E***, Delivery to NAcC of viral fluorescence-tagged ENT1 driven by an astrocytic promoter to test the impact of increased astrocyte-specific expression of ENT1 on DA release detected locally in NAcC. ***F***, Immunofluorescence for mCherry (top, red), mCherry-tagged ENT1 (bottom, red), and neuronal marker NeuN (cyan) in NAcC. Scale bars, 40 µm. ac, Anterior commissure. ***G***, Mean $[DA]_o$ transients (left) and corresponding mean peak $[DA]_o$ (right) evoked by a 1p or 5p at 50 Hz in NAcC in slices overexpressing ENT1 (ENT1-OX; red; $n = 9$ experiments/4 mice) or expressing control fluorophore mCherry (dark gray; $n = 8$ experiments/4 mice) under an astrocyte-specific promoter. ***H***, Summary of mean peak $[DA]_o$ before (gray) and after the application of A_1R antagonist CPT (10 μM) normalized to predrug baseline (dotted line; left) and right, corresponding mean $[DA]_o$ transients evoked by 1p and 5p at 50 Hz in NAcC in slices overexpressing ENT1 (ENT1-OX; red; $n = 9$ experiments/4 mice) or expressing control fluorophore mCherry (dark gray; $n = 8$ experiments/4 mice). ***I***, ***J***, Ratio of peak $[DA]_o$ evoked by 5p:1p ratio at 50 Hz (***I***) and Δ5p:1p ratio (***J***) before (light gray) and after application of CPT (10 μM) in slices overexpressing ENT1 (right, red) or expressing control fluorophore mCherry (left, dark gray). Data are summarized from ***H***. $p < 0.05$, $^{**}p < 0.01$, $^{***}p < 0.001$, unpaired t test (***A***, ***D***, ***G***, ***J***), two-way repeated-measures ANOVA (***B***, ***C***, ***H***, ***I***) with Sidak's multiple-comparisons test (***C***, ***I***). Error bars indicate SEM.

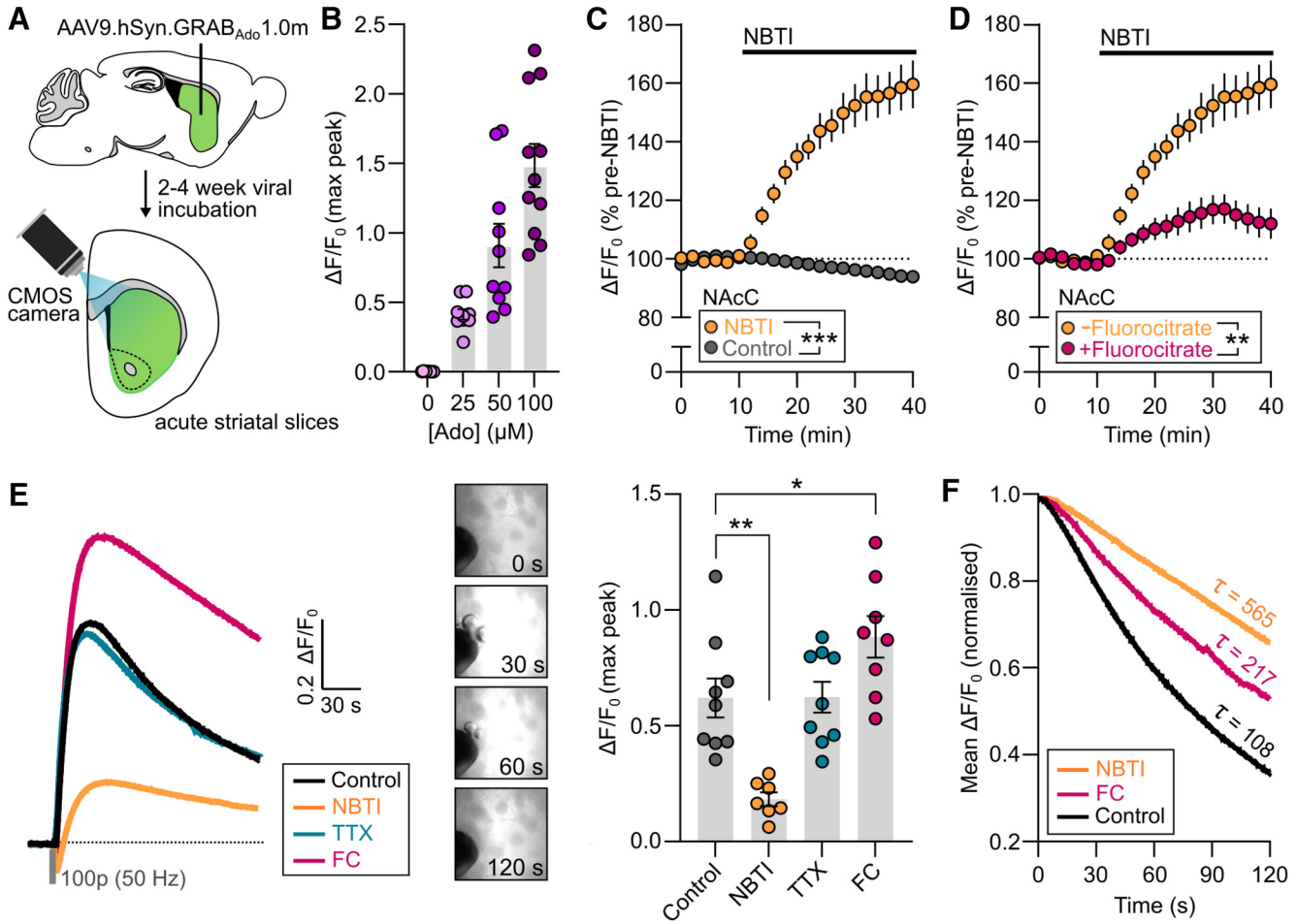

Figure 5. Striatal adenosine tone is regulated by ENT1 activity on striatal astrocytes. ***A***, Viral delivery of GRAB-Ado to striatum for imaging extracellular adenosine levels *ex vivo* in acute striatal slices. ***B***, Peak $\Delta F/F_0$ in response to increasing concentrations of exogenously applied adenosine (0–100 μM; $n = 9$–11 slices/4–6 mice). ***C***, Nonstimulated $\Delta F/F_0$ $GRAB_{Ado}$ signal in NAcC normalized to before drug application (dotted line) in control conditions (dark gray, $n = 10$ experiments/5 mice) or before and after application of NBTI (10 μM; orange, $n = 10$ experiments/5 mice). ***D***, As in ***C***, but in the presence of gliotoxin fluorocitrate (100 μM; pink, $n = 6$ experiments/4 mice). ***E***, Mean transients (left) and mean peak (right) $\Delta F/F_0$ $GRAB_{Ado}$ signal evoked by 100 electrical pulses (50 Hz) in drug-free control conditions ($n = 9$ slices/5 mice) or the presence of NBTI (10 μM; orange; $n = 7$ experiments/5 mice), TTX (1 μM; blue; $n = 9$ experiments/5 mice), or fluorocitrate (100 μM; pink; $n = 8$ experiments/5 mice). ***F***, Mean $\Delta F/F_0$ decay phase normalized to peak from ***E***. *$p < 0.05$, **$p < 0.01$, ***$p < 0.001$, two-way repeated-measures ANOVA (***C***, ***D***), and one-way ANOVA with Sidak's multiple-comparison test (***E***). Nonlinear regression with extra-sum-of-squares *F* test; τ = decay time constant (***F***). Error bars indicate SEM.

participate in this mechanism, we tested whether metabolic inhibition of astrocytes limited ENT1 function. We pretreated slices with the gliotoxin fluorocitrate (100 μM, for 45–60 min), which has been established to induce metabolic arrest in astrocytes, render them inactive, and prevent the effects of astrocytic transporters (Paulsen et al., 1987; Henneberger et al., 2010; Bonansco et al., 2011; Boddum et al., 2016; Roberts et al., 2020). The effects of ENT1 inhibitor NBTI on GRAB-Ado fluorescence were occluded after pretreatment with fluorocitrate (Fig. 5*D*; $F_{(1,14)} = 14.32$, $p = 0.002$, two-way RM ANOVA: main effect of FC).

To further characterize and validate the role of ENT1 and astrocytes in striatal adenosine signaling, we explored their impact on the dynamics of extracellular adenosine transients evoked electrically by trains of electrical stimulation (100 pulses, 50 Hz; Fig. 5*E*). Evoked increases in extracellular adenosine concentrations exhibited relatively extended rise times (~30 s) and clearance times, as reported previously in cultured hippocampal neurons and acute hippocampal and medial prefrontal cortex mouse brain slices (Wu et al., 2020), and surprisingly release was activated via a mechanism that was not prevented by Na_v blocker TTX (1 μM). (Fig. 5*E*; $F_{(3,29)} = 13.60$, $p < 0.0001$, one-way ANOVA; TTX vs control: $p > 0.99$, Sidak's multiple comparisons). In slices pretreated with the ENT1 inhibitor NBTI (10 μM, for 45–60 min), the peak of evoked adenosine levels was attenuated (Fig. 5*E*; $F_{(3,29)} = 13.60$, $p < 0.0001$, one-way ANOVA; NBTI vs control: $p = 0.001$, Sidak's multiple comparisons), but the clearance time constant was extended (Fig. 5*F*; $F = 8543$, $p < 0.0001$, extra-sum-of-squares *F* test; control, τ = 108.4; NBTI, τ = 564.5), indicating reduced release and uptake, and seen previously in cultured hippocampal neurons (Wu et al., 2020). In slices pretreated with the gliotoxin fluorocitrate (100 μM, for 45–60 min), both the peak level of adenosine and the time constant for clearance were elevated (Fig. 5*E*; $F_{(3,29)} = 13.60$, $p < 0.0001$, one-way ANOVA; FC vs control: $p = 0.049$, Sidak's multiple comparisons; Fig. 5*F*; $F = 8543$, $p < 0.0001$, extra-sum-of-squares *F* test; control, τ = 108.4; FC, τ = 217.0), indicating that ENT1 on astrocytes supports adenosine uptake.

EtOH increases tonic A_1R-mediated inhibition of DA release

Our data indicate that astrocytic ENT1 function regulates tonic A_1R-mediated inhibition of DA output in NAcC. Acute exposure to ethanol is documented to increase extracellular adenosine levels in many brain nuclei, including striatum, via inhibition of

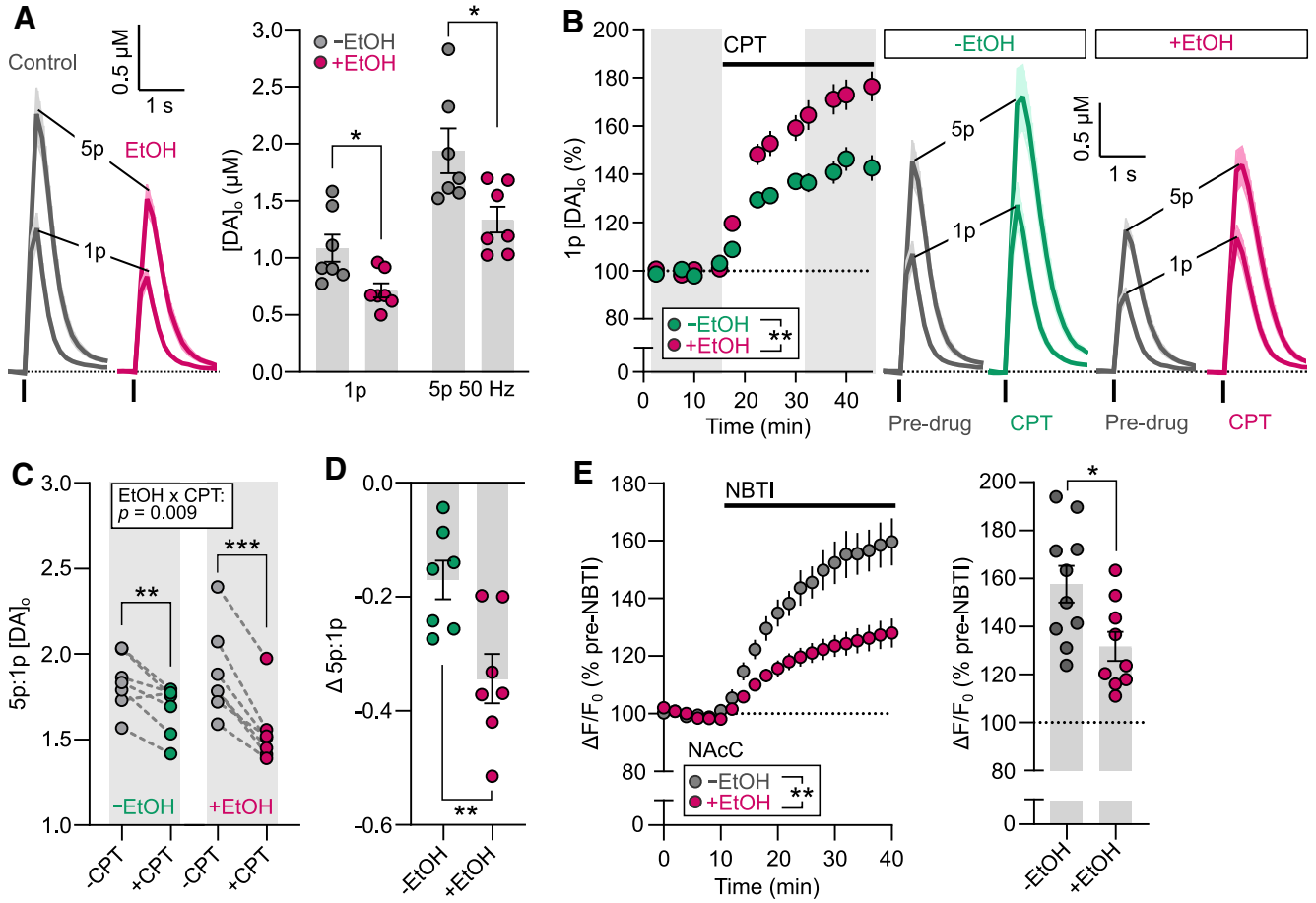

Figure 6. EtOH enhances tonic adenosine A_1R-mediated inhibition of DA release. ***A***, Mean $[DA]_o$ transients (left) and corresponding mean peak $[DA]_o$ (right) evoked by 1p or 5p at 50 Hz in NAcC in the absence (gray; $n = 7$ experiments/4 mice) or presence of 50 mM EtOH (pink; $n = 7$ experiments/4 mice). ***B***, Summary of mean peak $[DA]_o$ before (gray) and after application of A_1R antagonist CPT (10 μM) normalized to predrug baseline level (dotted line; left) and right, corresponding mean $[DA]_o$ transients evoked by 1p and 5p at 50 Hz in NAcC in the absence (green, $n = 7$ experiments/4 mice) or presence of 50 mM EtOH (pink; $n = 7$ experiments/4 mice). ***C***, ***D***, Ratio of peak $[DA]_o$ evoked by 5p:1p ratio at 50 Hz (***C***) and Δ5p:1p ratio (***D***) before (gray) and after application of CPT (10 μM) in the absence (left, green) or presence of 50 mM EtOH (right, pink). Data are summarized from ***B***. ***E***, Summary (left) and mean peak (right) of unstimulated $\Delta F/F_0$ GRAB-Ado signal in NAcC normalized to predrug baseline (dotted line) before and after the application of ENT1 inhibitor NBTI (10 μM) in the absence (gray; $n = 10$ experiments/5 mice) or presence of 50 mM EtOH (pink; $n = 9$ experiments/5 mice). $^*p < 0.05$, $^{**}p < 0.01$, $^{***}p < 0.001$, unpaired *t* test (***A***, ***D***), two-way repeated-measures ANOVA (***B***, ***C***, ***E***) with Sidak's multiple comparisons (***C***). Error bars indicate SEM.

adenosine uptake by ENT1 (Nagy et al., 1989, 1990; Choi et al., 2004). Given that ethanol also attenuates evoked DA release in NAc (Yorgason et al., 2014, 2015; Karkhanis et al., 2015; Rose et al., 2016), we tested whether acute ethanol exposure might increase tonic A_1R-mediated inhibition of DA release via impaired ENT1 function. We pretreated slices with ethanol (2–3 h), at a concentration (50 mM) that correlates to a blood alcohol concentration of 230 mg/dl in humans and is consistent with what late-stage alcoholics achieve (Brick and Erickson, 2009). We first confirmed that pretreating slices with ethanol using this paradigm reduced $[DA]_o$ evoked by single and five pulses (50 Hz) of electrical stimulation in NAcC (Fig. 6*A*; 1p: $t_{(12)} = 2.74$, $p = 0.018$; 5p: $t_{(12)} = 2.67$, $p = 0.020$; unpaired *t* tests). Next, we found that the effect of A_1R antagonism with CPT (10 μM) on $[DA]_o$ evoked by single electrical pulses was elevated compared with control slices (Fig. 6*B*; $F_{(1,12)} = 18.04$, $p = 0.0011$, two-way RM ANOVA: main effect of drug). A_1 receptor antagonism with CPT decreased the ratio of $[DA]_o$ evoked by 5p:1p ratio (50 Hz; Fig. 6*C*; $F_{(1,12)} = 68.51$, $p < 0.0001$, two-way RM ANOVA: main effect of drug), and there was a significant interaction between ethanol and CPT (Fig. 6*C*; $F_{(1,12)} = 9.36$, $p = 0.0099$, two-way RM ANOVA: ethanol × CPT interaction), which was borne out by a more pronounced decrease after ethanol than in control slices (Fig. 6*D*; $t_{(12)} = 3.16$, $p = 0.0082$, unpaired *t* test). To test directly whether ethanol in this paradigm impaired adenosine uptake by ENT1, we imaged tonic extracellular adenosine levels with the GRAB-Ado sensor during application of ENT1 inhibitor NBTI (10 μM). NBTI increased tonic extracellular adenosine levels in NAcC to a significantly lesser degree in slices preincubated with ethanol than in controls (Fig. 6*E*; $F_{(1,17)} = 11.30$, $p = 0.0037$, two-way RM ANOVA: main effect of drug; $t_{(17)} = 2.60$, $p = 0.019$, unpaired *t* test). These data indicate that tonic A_1R-mediated inhibition of DA axons by adenosine in the NAcC is elevated by acute ethanol exposure, paralleled by an underlying attenuated uptake of adenosine uptake by ENT1.

Discussion

Here, we reveal that DA release in NAcC is under a tonic inhibition by ambient adenosine levels acting at A_1Rs, and that ENT1, located at least in part on striatal astrocytes, governs the level of this tonic inhibition. Moreover, we reveal that ethanol promotes A_1R inhibition of DA release, through elevating adenosine levels

by diminishing adenosine uptake via ENT1. These data support the emerging concept that astrocytes play important roles in setting the level of striatal DA output, in health and disease.

Direct versus indirect actions of A_1Rs

Our data provide functional evidence for direct regulation of DA release by A_1Rs. Immunocytochemical studies in rat striatal synaptosomes indicate that dopaminergic axons can contain A_1Rs (Borycz et al., 2007), but direct immunocytochemical evidence *in situ* is currently lacking. We excluded indirect actions of A_1Rs via key candidate pathways, namely cholinergic inputs that act via nAChRs, and GABAergic networks that act via $GABA_A$/$GABA_B$ receptors on DA axons. Previous reports have excluded effects of glutamatergic modulation (Borycz et al., 2007; O'Connor and O'Neill, 2008). Moreover, we found that A_1R agonists inhibited DA release evoked by even single short optogenetic stimulation of ChR2-expressing DA axons, which should not coactivate other striatal neurons, suggesting that the locations for A_1Rs that regulate DA are either a currently undisclosed tonically active cell type with currently unknown actions on DA or, more parsimoniously, DA axons themselves.

Tonic inhibition

A_1R antagonists enhanced DA release evoked by single short optogenetic stimulation, suggesting that A_1R activation does not require stimulation of any other network, and is tonically activated by an ambient striatal adenosine tone. An adenosine tone at striatal A_1Rs has previously been described on glutamate inputs in NAcC (Brundege and Williams, 2002; Choi et al., 2004). Extracellular adenosine concentrations in the brain have been suggested to be in the range of 25–250 nM under basal conditions, which are sufficient to activate high-affinity A_1Rs (Dunwiddie and Masino, 2001). In further support for a resting adenosine tone in NAcC, we could detect extracellular adenosine with the GRAB-Ado sensor, following application of an ENT1 inhibitor, in the absence of any striatal stimulation. The source of adenosine is still undetermined, but can arise from the catabolism of ATP from neuronal and non-neuronal sources (Latini and Pedata, 2001), including astrocytes (Corkrum et al., 2020).

A_1Rs modify DA signal contrast for firing frequency

We found that A_1R activation not only limits the overall amplitude of DA output, but also promotes the contrast in DA signals released by different firing rates and pulse numbers, and, vice versa, that A_1R antagonists reduce this contrast. The strength of A_1R-mediated inhibition of DA release varied with adenosine concentration, resulting from ENT1 inhibition or overexpression, and, furthermore, was greater for lower frequencies of activation of DA axons. These data indicate that an adenosine tone preferentially limits DA output during the lower frequencies of DA neuron activity that represent tonic activity, while leaving relatively intact the DA release evoked by the higher frequencies associated with phasic activity in DA neurons. The preferential inhibition of DA release by low frequencies of activity parallels the effects of GABA input to DA axons (Lopes et al., 2019; Roberts et al., 2020, 2021) and could indicate a preferential influence of striatal adenosine on DA functions that are proposed to be mediated by low frequencies of activity (e.g., the ongoing monitoring of reward value and its changes; Wang et al., 2021). We identified an underlying change in the dynamic short-term plasticity (STP) of DA output that corresponds to this change to frequency filtering, which again parallels the effect of GABA on STP in DA release (Lopes et al., 2019; Roberts et al., 2020). Elsewhere in the brain, A_1R activation, including through ambient adenosine, can modulate STP of glutamate transmission through a presynaptic mechanism (Moore et al., 2003; Wong et al., 2006; Yang et al., 2007; Qi et al., 2017; Perrier et al., 2019). A_1Rs are $G_{i/o}$ coupled, and so their activation causes the inhibition of adenylyl cyclase, the activation of potassium channels, and the inactivation of voltage-gated calcium channels (VGCCs; Haas and Selbach, 2000). We have recently revealed that mechanisms that determine axonal excitability, particularly potassium-dependent processes, strongly gate STP of DA release (Condon et al., 2019), while calcium largely gates amplitude. We therefore hypothesize that A_1Rs on striatal DA axons likely inhibit the overall amplitude of DA release via reduced VGCC activity while simultaneously gating the STP of DA release by modifying axonal excitability via potassium-dependent conductances. Future studies are needed to establish these potential mechanisms.

ENT1 and astrocytes are key regulators of tonic A_1R inhibition of DA release

We established that ENT1 in NAcC limits ambient adenosine levels and tonic A_1R inhibition of DA axons, and thereby indirectly facilitates DA release. ENT1 usually facilitates adenosine uptake from the extracellular milieu, but can reverse to release adenosine (Parkinson et al., 2011), and ENT1 has been shown to facilitate adenosine release evoked by electrical stimulation in cultured hippocampal neurons (Wu et al., 2020). Intriguingly, we found that adenosine release driven by electrical stimulation was TTX insensitive and sensitive to ENT1 inhibition. Together, our data show that ambient adenosine in NAcC is limited by uptake via ENT1 but can be released via ENT1 reversal in some conditions. There is an additional ENT in striatum, ENT2 (Jennings et al., 2001; Anderson et al., 1999), whose roles we did not explore. ENT1 is thought to be responsible for the majority of adenosine transport and, subsequently, the key regulator of extracellular adenosine levels across the brain (Young et al., 2008).

We found a major role for ENT1 located in striatal astrocytes, although we did not test or exclude roles for ENT1 located on neurons. The glial metabolic poison fluorocitrate limited the effects of ENT1 inhibitors on adenosine tone, while overexpressing ENT1 in astrocytes boosted evoked DA release by limiting tonic A_1R inhibition. This strategy for viral overexpression of ENT1 in striatal astrocytes has previously been shown to increase ENT1 expression by ~30%, but also increases striatal GFAP expression and modifies astrocyte morphology (Hong et al., 2020). ENT1 expression has also been shown to regulate astrocyte-specific excitatory amino acid transporter 2 (EAAT2) and aquaporin-4 expression in NAcC (Wu et al., 2010; Lee et al., 2013). These additional astrocyte-specific modifications might also contribute to boosted DA signaling in NAcC, beyond mechanisms involving tonic inhibition by adenosine tone. Regardless, astrocytic ENT1 in striatum has previously been reported to play key roles in reward-seeking behaviors (Hong et al., 2020; Kang et al., 2020), which our data suggest could be mediated by underlying changes to DA signaling.

The role for ENT1 on astrocytes in gating DA output parallels our recent finding that GABA transporters (GAT1 and GAT3) on astrocytes in dorsal striatum set the level of tonic GABAergic inhibition of DA release (Roberts et al., 2020). Furthermore, EAAT2, enriched on astrocytes, limits glutamate-mediated inhibition of DA release (Zhang and Sulzer, 2003), and, thus, our collective findings point to astrocytic transporters across neurotransmitter categories as regulators of DA release.

Dysregulation of A_1R inhibition of DA release by ethanol

To probe the wider potential significance of the regulation of DA in NAcC by adenosine tone and ENT1, we explored whether A_1R inhibition of DA release was modified by ethanol. Ethanol has been shown to increase extracellular adenosine levels by impairing adenosine uptake via ENT1 after acute exposure (Nagy et al., 1989, 1990; Choi et al., 2004) and, separately, to reduce DA release following acute application (Yorgason et al., 2014, 2015) or following chronic intermittent exposure in mice (Karkhanis et al., 2015; Rose et al., 2016). Here we bridge these different findings by revealing that ethanol can reduce DA output via a boosted tonic A_1R inhibition. While pretreating slices with 50 mM ethanol to understand the disruption to cellular and circuit function has limitations in informing effects on behavior, we speculate that this mechanism could help to explain how striatal A_1Rs contribute to the ataxic and hypnotic effects of ethanol (Meng and Dar, 1995; Phan et al., 1997; Dar, 2001), as well as how acute ethanol exposure attenuates concurrent GABA corelease from DA axons in dorsal striatum (Kim et al., 2015).

Chronic ethanol exposure is thought to evoke an adaptive response, resulting in decreased ENT1 expression, and therefore a reduced ability for ethanol to increase extracellular adenosine (Nagy et al., 1989). Indeed, rats permitted daily access to ethanol for 8 weeks exhibit downregulated ENT1 gene expression in NAc (Bell et al., 2009). ENT1-null mice exhibit reduced hypnotic and ataxic responses to ethanol, increased ethanol consumption, and decreased adenosine tone in NAc, while viral-mediated rescue of ENT1 expression in NAc reduces ethanol consumption (Choi et al., 2004; Jia et al., 2020). Furthermore, growing evidence implicates striatal adenosine signaling in the neurobiological adaptations of other drugs of abuse (Bachtell, 2017; Ballesteros-Yáñez et al., 2018). Repeated cocaine administration enhances adenosine uptake, reduces adenosine tone, and reduces plasma membrane A_1R expression in NAcC (Manzoni et al., 1998; Toda et al., 2003), while striatal μ-opioid receptor activation by opioids results in reduced striatal adenosine tone in dorsomedial striatum (Adhikary and Birdsong, 2021). Dysregulated tonic A_1R inhibition of glutamate afferents in NAc is thought to be a key circuit adaptation underlying ethanol abuse and other drugs of abuse (Choi et al., 2004; Chen et al., 2010; Wu et al., 2010; Nam et al., 2011); however, given the role that adenosine tone plays in setting the level and activity dependence of DA output we describe here, we speculate that dysregulated tonic A_1R inhibition of DA release in NAcC might also be an important circuit adaptation underlying drug abuse.

In conclusion, we show here that A_1Rs can tonically inhibit DA output though an ambient adenosine tone, and that A_1Rs additionally regulate the activity sensitivity of DA release, preferentially impacting on release by low frequencies. Furthermore, we find that tonic A_1R inhibition of DA release is regulated by ENT1 and astrocytes, and is dysregulated by ethanol. These data provide a further mechanism through which ethanol modulates striatal DA function and corroborates emerging data highlighting astrocytic transporters as important regulators of striatal function.

References

Adhikary S, Birdsong WT (2021) μ opioid receptors acutely regulate adenosine signaling in a thalamo-striatal circuit. bioRxiv. doi: 10.1101/2021.05.25.445648.

Alexander SP, Reddington M (1989) The cellular localization of adenosine receptors in rat neostriatum. Neuroscience 28:645–651.

Anderson CM, Xiong W, Geiger JD, Young JD, Cass CE, Baldwin SA, Parkinson FE (1999) Distribution of equilibrative, nitrobenzylthioinosine-sensitive nucleoside transporters (ENT1) in brain. J Neurochem 73:867–873.

Bachtell RK (2017) Cocaine addiction and adenosine A1 and A2A receptors. In: The neuroscience of cocaine: mechanisms and treatment (Preedy VR, ed), pp 429–437. London: Elsevier.

Ballesteros-Yáñez I, Castillo CA, Merighi S, Gessi S (2018) The role of adenosine receptors in psychostimulant addiction. Front Pharmacol 8:985.

Bell RL, Kimpel MW, McClintick JN, Strother WN, Carr LG, Liang T, Rodd ZA, Mayfield RD, Edenberg HJ, McBride WJ (2009) Gene expression changes in the nucleus accumbens of alcohol-preferring rats following chronic ethanol consumption. Pharmacol Biochem Behav 94:131–147.

Boddum K, Jensen TP, Magloire V, Kristiansen U, Rusakov DA, Pavlov I, Walker MC (2016) Astrocytic GABA transporter activity modulates excitatory neurotransmission. Nat Commun 7:13572.

Bonansco C, Couve A, Perea G, Ferradas CA, Roncagliolo M, Fuenzalida M (2011) Glutamate released spontaneously from astrocytes sets the threshold for synaptic plasticity. Eur J Neurosci 33:1483–1492.

Borycz J, Pereira MF, Melani A, Rodrigues RJ, Köfalvi A, Panlilio L, Pedata F, Goldberg SR, Cunha RA, Ferré S (2007) Differential glutamate-dependent and glutamate-independent adenosine A_1 receptor-mediated modulation of dopamine release in different striatal compartments. J Neurochem 101:355–363.

Brick J, Erickson CK (2009) Intoxication is not always visible: an unrecognized prevention challenge. Alcohol Clin Exp Res 33:1489–1507.

Britt JP, McGehee DS (2008) Presynaptic opioid and nicotinic receptor modulation of dopamine overflow in the nucleus accumbens. J Neurosci 28:1672–1681.

Brown SJ, James S, Reddington M, Richardson PJ (1990) Both A1 and A2a purine receptors regulate striatal acetylcholine release. J Neurochem 55:31–38.

Brundege JM, Williams JT (2002) Differential modulation of nucleus accumbens synapses. J Neurophysiol 88:142–151.

Chai H, Diaz-Castro B, Shigetomi E, Monte E, Octeau JC, Yu X, Cohn W, Rajendran PS, Vondriska TM, Whitelegge JP, Coppola G, Khakh BS (2017) Neural circuit-specialized astrocytes: transcriptomic, proteomic, morphological, and functional evidence. Neuron 95:531–549.

Cheffer A, Castillo ARG, Corrêa-Velloso J, Gonçalves MCB, Naaldijk Y, Nascimento IC, Burnstock G, Ulrich H (2018) Purinergic system in psychiatric diseases. Mol Psychiatry 23:94–106.

Chen J, Nam HW, Lee MR, Hinton DJ, Choi S, Kim T, Kawamura T, Janak PH, Choi DS (2010) Altered glutamatergic neurotransmission in the striatum regulates ethanol sensitivity and intake in mice lacking ENT1. Behav Brain Res 208:636–642.

Choi DS, Cascini MG, Mailliard W, Young H, Paredes P, McMahon T, Diamond I, Bonci A, Messing RO (2004) The type 1 equilibrative nucleoside transporter regulates ethanol intoxication and preference. Nat Neurosci 7:855–861.

Condon MD, Platt NJ, Zhang YF, Roberts BM, Clements MA, Vietti-Michelina S, Tseu MY, Brimblecombe KR, Threlfell S, Mann EO, Cragg SJ (2019) Plasticity in striatal dopamine release is governed by release-independent depression and the dopamine transporter. Nat Commun 10:4263.

Corkrum M, Covelo A, Lines J, Bellocchio L, Pisansky M, Loke K, Quintana R, Rothwell PE, Lujan R, Marsicano G, Martin ED, Thomas MJ, Kofuji P, Araque A (2020) Dopamine-evoked synaptic regulation in the nucleus accumbens requires astrocyte activity. Neuron 105:1036–1047.

Dar MS (2001) Modulation of ethanol-induced motor incoordination by mouse striatal A1 adenosinergic receptor. Brain Res Bull 55:513–520.

Dunwiddie TV, Masino SA (2001) The role and regulation of adenosine in the central nervous system. Annu Rev Neurosci 24:31–55.

Ferré S, O'Connor WT, Svenningsson P, Björklund L, Lindberg J, Tinner B, Strömberg I, Goldstein M, Ögren SO, Ungerstedt U, Fredholm BB, Fuxe K (1996) Dopamine D1 receptor-mediated facilitation of GABAergic neurotransmission in the rat strioentropeduncular pathway and its modulation by adenosine A1 receptor-mediated mechanisms. Eur J Neurosci 8:1545–1553.

Haas HL, Selbach O (2000) Functions of neuronal adenosine receptors. Naunyn Schmiedebergs Arch Pharmacol 362:375–381.

Hartung H, Threlfell S, Cragg SJ (2011) Nitric oxide donors enhance the frequency dependence of dopamine release in nucleus accumbens. Neuropsychopharmacology 36:1811–1822.

Henneberger C, Papouin T, Oliet SHR, Rusakov DA (2010) Long-term potentiation depends on release of d-serine from astrocytes. Nature 463:232–236.

Hong S, Bullert A, Baker M, Choi D (2020) Astrocytic equilibrative nucleoside transporter type 1 upregulations in the dorsomedial and dorsolateral striatum distinctly coordinate goal-directed and habitual ethanol-seeking behaviours in mice. Eur J Neurosci 52:3110–3123.

Jennings LL, Hao C, Cabrita MA, Vickers MF, Baldwin SA, Young JD, Cass CE (2001) Distinct regional distribution of human equilibrative nucleoside transporter proteins 1 and 2 (hENT1 and hENT2) in the central nervous system. Neuropharmacology 40:722–731.

Jia YF, Vadnie CA, Ho AMC, Peyton L, Veldic M, Wininger K, Matveyenko A, Choi DS (2020) Type 1 equilibrative nucleoside transporter (ENT1) regulates sex-specific ethanol drinking during disruption of circadian rhythms. Addict Biol 25:e12801.

Jones IW, Bolam JP, Wonnacott S (2001) Presynaptic localisation of the nicotinic acetylcholine receptor $\beta 2$ subunit immunoreactivity in rat nigrostriatal dopaminergic neurones. J Comp Neurol 439:235–247.

Kang S, Hong SI, Lee J, Peyton L, Baker M, Choi S, Kim H, Chang SY, Choi DS (2020) Activation of astrocytes in the dorsomedial striatum facilitates transition from habitual to goal-directed reward-seeking behavior. Biol Psychiatry 88:797–808.

Karkhanis AN, Rose JH, Huggins KN, Konstantopoulos JK, Jones SR (2015) Chronic intermittent ethanol exposure reduces presynaptic dopamine neurotransmission in the mouse nucleus accumbens. Drug Alcohol Depend 150:24–30.

Kim JI, Ganesan S, Luo SX, Wu YW, Park E, Huang EJ, Chen L, Ding JB (2015) Aldehyde dehydrogenase 1a1 mediates a GABA synthesis pathway in midbrain dopaminergic neurons. Science 350:102–106.

Kosillo P, Zhang Y-F, Threlfell S, Cragg SJ (2016) Cortical control of striatal dopamine transmission via striatal cholinergic interneurons. Cereb Cortex 26:4160–4169.

Latini S, Pedata F (2001) Adenosine in the central nervous system: release mechanisms and extracellular concentrations. J Neurochem 79:463–484.

Lee MR, Ruby CL, Hinton DJ, Choi S, Adams CA, Young Kang N, Choi DS (2013) Striatal adenosine signaling regulates EAAT2 and astrocytic AQP4 expression and alcohol drinking in mice. Neuropsychopharmacology 38:437–445.

Lemos JC, Shin JH, Alvarez VA (2019) Striatal cholinergic interneurons are a novel target of corticotropin releasing factor. J Neurosci 39:5647–5661.

Lopes EF, Roberts BM, Siddorn RE, Clements MA, Cragg SJ (2019) Inhibition of nigrostriatal dopamine release by striatal $GABA_A$ and $GABA_B$ receptors. J Neurosci 39:1058–1065.

Manzoni O, Pujalte D, Williams J, Bockaert J (1998) Decreased presynaptic sensitivity to adenosine after cocaine withdrawal. J Neurosci 18:7996–8002.

Melchior JR, Ferris MJ, Stuber GD, Riddle DR, Jones SR (2015) Optogenetic versus electrical stimulation of dopamine terminals in the nucleus accumbens reveals local modulation of presynaptic release. J Neurochem 134:833–844.

Meng Z-H, Dar MS (1995) Possible role of striatal adenosine in the modulation of acute ethanol-induced motor incoordination in rats. Alcohol Clin Exp Res 19:892–901.

Moore KA, Nicoll RA, Schmitz D (2003) Adenosine gates synaptic plasticity at hippocampal mossy fiber synapses. Proc Natl Acad Sci U S A 100:14397–14402.

Nagai K, Nagasawa K, Fujimoto S (2005) Transport mechanisms for adenosine and uridine in primary-cultured rat cortical neurons and astrocytes. Biochem Biophys Res Commun 334:1343–1350.

Nagy LE, Diamond I, Collier K, Lopez L, Ullman B, Gordon AS (1989) Adenosine is required for ethanol-induced heterologous desensitization. Mol Pharmacol 36:744–748.

Nagy LE, Diamond I, Casso DJ, Franklin C, Gordon AS (1990) Ethanol increases extracellular adenosine by inhibiting adenosine uptake via the nucleoside transporter. J Biol Chem 265:1946–1951.

Nam HW, Lee MR, Zhu Y, Wu J, Hinton DJ, Choi S, Kim T, Hammack N, Yin JCP, Choi DS (2011) Type 1 equilibrative nucleoside transporter regulates ethanol drinking through accumbal *N*-methyl-D-aspartate receptor signaling. Biol Psychiatry 69:1043–1051.

Nguyen MD, Ross AE, Ryals M, Lee ST, Venton BJ (2015) Clearance of rapid adenosine release is regulated by nucleoside transporters and metabolism. Pharmacol Res Perspect 3:e00189.

Nolan SO, Zachry JE, Johnson AR, Brady LJ, Siciliano CA, Calipari ES (2020) Direct dopamine terminal regulation by local striatal microcircuitry. J Neurochem 155:475–493.

O'Connor J, O'Neill C (2008) A role for adenosine A1 receptors in GABA and NMDA-receptor mediated modulation of dopamine release: studies using fast cyclic voltammetry. Sensors 8:5516–5534.

O'Neill C, Nolan BJ, Macari A, O'Boyle KM, O'Connor JJ (2007) Adenosine A1 receptor-mediated inhibition of dopamine release from rat striatal slices is modulated by D1 dopamine receptors. Eur J Neurosci 26:3421–3428.

Okada M, Mizuno K, Kaneko S (1996) Adenosine A1 and A2 receptors modulate extracellular dopamine levels in rat striatum. Neurosci Lett 212:53–56.

Pajski ML, Venton BJ (2010) Adenosine release evoked by short electrical stimulations in striatal brain slices is primarily activity dependent. ACS Chem Neurosci 1:775–787.

Parkinson FE, Damaraju VL, Graham K, Yao SYM, Baldwin SA, Cass CE, Young JD (2011) Molecular biology of nucleoside transporters and their distributions and functions in the brain. Curr Top Med Chem 11:948–972.

Paulsen RE, Contestabile A, Villani L, Fonnum F (1987) An in vivo model for studying function of brain tissue temporarily devoid of glial cell metabolism: the use of fluorocitrate. J Neurochem 48:1377–1385.

Peng L, Huang R, Yu ACH, Fung KY, Rathbone MP, Hertz L (2005) Nucleoside transporter expression and function in cultured mouse astrocytes. Glia 52:25–35.

Peng W, Wu Z, Song K, Zhang S, Li Y, Xu M (2020) Regulation of sleep homeostasis mediator adenosine by basal forebrain glutamatergic neurons. Science 369:eabb0556.

Perrier SP, Gleizes M, Fonta C, Nowak LG (2019) Effect of adenosine on short-term synaptic plasticity in mouse piriform cortex in vitro: adenosine acts as a high-pass filter. Physiol Rep 7:e13992.

Phan TA, Gray AM, Nyce JW (1997) Intrastriatal adenosine A1 receptor antisense oligodeoxynucleotide blocks ethanol-induced motor incoordination. Eur J Pharmacol 323:R5–R7.

Preston Z, Lee K, Widdowson L, Freeman TC, Dixon AK, Richardson PJ (2000) Adenosine receptor expression and function in rat striatal cholinergic interneurons. Br J Pharmacol 130:886–890.

Qi G, Van Aerde K, Abel T, Feldmeyer D (2017) Adenosine differentially modulates synaptic transmission of excitatory and inhibitory microcircuits in layer 4 of rat barrel cortex. Cereb Cortex 27:4411–4422.

Quarta D, Ferré S, Solinas M, You ZB, Hockemeyer J, Popoli P, Goldberg SR (2004a) Opposite modulatory roles for adenosine A1 and A2A receptors on glutamate and dopamine release in the shell of the nucleus accumbens. Effects of chronic caffeine exposure. J Neurochem 88:1151–1158.

Quarta D, Borycz J, Solinas M, Patkar K, Hockemeyer J, Ciruela F, Lluis C, Franco R, Woods AS, Goldberg SR, Ferré S (2004b) Adenosine receptor-mediated modulation of dopamine release in the nucleus accumbens depends on glutamate neurotransmission and N-methyl-D-aspartate receptor stimulation. J Neurochem 91:873–880.

Rice ME, Cragg SJ (2004) Nicotine amplifies reward-related dopamine signals in striatum. Nat Neurosci 7:583–584.

Rice ME, Patel JC, Cragg SJ (2011) Dopamine release in the basal ganglia. Neuroscience 198:112–137.

Richardson PJ, Brown SJ (1987) ATP release from affinity-purified rat cholinergic nerve terminals. J Neurochem 48:622–630.

Roberts BM, Doig NM, Brimblecombe KR, Lopes EF, Siddorn RE, Threlfell S, Connor-Robson N, Bengoa-Vergniory N, Pasternack N, Wade-Martins R, Magill PJ, Cragg SJ (2020) GABA uptake transporters support dopamine release in dorsal striatum with maladaptive downregulation in a parkinsonism model. Nat Commun 11:4958.

Roberts BM, Lopes EF, Cragg SJ (2021) Axonal modulation of striatal dopamine release by local γ-aminobutyric acid (GABA) signalling. Cells 10:709.

Rose JH, Karkhanis AN, Chen R, Gioia D, Lopez MF, Becker HC, McCool BA, Jones SR (2016) Supersensitive kappa opioid receptors promotes ethanol withdrawal-related behaviors and reduce dopamine signaling in the nucleus accumbens. Int J Neuropsychopharmacol 19:pyv127.

Ross AE, Venton BJ (2015) Adenosine transiently modulates stimulated dopamine release in the caudate-putamen via A1 receptors. J Neurochem 132:51–60.

Solinas M, Ferré S, You ZB, Karcz-Kubicha M, Popoli P, Goldberg SR (2002) Caffeine induces dopamine and glutamate release in the shell of the nucleus accumbens. J Neurosci 22:6321–6324.

Song WJ, Tkatch T, Surmeier DJ (2000) Adenosine receptor expression and modulation of Ca^{2+} channels in rat striatal cholinergic interneurons. J Neurophysiol 83:322–332.

Stouffer MA, Woods CA, Patel JC, Lee CR, Witkovsky P, Bao L, Machold RP, Jones KT, de Vaca SC, Reith MEA, Carr KD, Rice ME (2015) Insulin enhances striatal dopamine release by activating cholinergic interneurons and thereby signals reward. Nat Commun 6:8543.

Sulzer D, Cragg SJ, Rice ME (2016) Striatal dopamine neurotransmission: regulation of release and uptake. Basal Ganglia 6:123–148.

Tanaka A, Nishida K, Okuda H, Nishiura T, Higashi Y, Fujimoto S, Nagasawa K (2011) Peroxynitrite treatment reduces adenosine uptake via the equilibrative nucleoside transporter in rat astrocytes. Neurosci Lett 498:52–56.

Threlfell S, Lalic T, Platt NJ, Jennings KA, Deisseroth K, Cragg SJ (2012) Striatal dopamine release is triggered by synchronized activity in cholinergic interneurons. Neuron 75:58–64.

Toda S, Alguacil LF, Kalivas PW (2003) Repeated cocaine administration changes the function and subcellular distribution of adenosine A1 receptor in the rat nucleus accumbens. J Neurochem 87:1478–1484.

Wang Y, Toyoshima O, Kunimatsu J, Yamada H, Matsumoto M (2021) Tonic firing mode of midbrain dopamine neurons continuously tracks reward values changing moment-by-moment. eLife 10:e63166.

Wong AYC, Billups B, Johnston J, Evans RJ, Forsythe ID (2006) Endogenous activation of adenosine A1 receptors, but not P2X receptors, during high-frequency synaptic transmission at the calyx of held. J Neurophysiol 95:3336–3342.

Wu J, Lee MR, Choi S, Kim T, Choi D-S (2010) ENT1 regulates ethanol-sensitive EAAT2 expression and function in astrocytes. Alcohol Clin Exp Res 34:1110–1117.

Wu Z, Cui Y, Wang H, Song K, Yuan Z, Dong A, Wu H, Wan Y, Pan S, Peng W, Jing M, Xu M, Luo M, Li Y (2020) A GRAB sensor reveals activity-dependent non-vesicular somatodendritic adenosine release. bioRxiv. doi: 10.1101/2020.05.04.075564.

Yang SC, Chiu TH, Yang HW, Min MY (2007) Presynaptic adenosine A1 receptors modulate excitatory synaptic transmission in the posterior piriform cortex in rats. Brain Res 1156:67–79.

Yorgason JT, Ferris MJ, Steffensen SC, Jones SR (2014) Frequency-dependent effects of ethanol on dopamine release in the nucleus accumbens. Alcohol Clin Exp Res 38:438–447.

Yorgason JT, Rose JH, McIntosh JM, Ferris MJ, Jones SR (2015) Greater ethanol inhibition of presynaptic dopamine release in C57BL/6J than DBA/2J mice: role of nicotinic acetylcholine receptors. Neuroscience 284:854–864.

Young JD, Yao SYM, Sun L, Cass CE, Baldwin SA (2008) Human equilibrative nucleoside transporter (ENT) family of nucleoside and nucleobase transporter proteins. Xenobiotica 38:995–1021.

Zhang H, Sulzer D (2003) Glutamate spillover in the striatum depresses dopaminergic transmission by activating group I metabotropic glutamate receptors. J Neurosci 23:10585–10592.

Zhang H, Sulzer D (2004) Frequency-dependent modulation of dopamine release by nicotine. Nat Neurosci 7:581–582.